Biol Cybern (2008) 98:519–539
DOI 10.1007/s00422-008-0213-5

ORIGINAL PAPER

Biological Cybernetics

Electric imaging through active electrolocation: implication for the analysis of complex scenes

Jacob Engelmann · João Bacelo · Michael Metzen · Roland Pusch · Beatrice Bouton · Adriana Migliaro · Angel Caputi · Ruben Budelli · Kirsty Grant · Gerhard von der Emde

Received: 12 November 2007 / Accepted: 29 January 2008

Abstract The electric sense of mormyrids is often regarded as an adaptation to conditions unfavourable for vision and in these fish it has become the dominant sense for active orientation and communication tasks. With this sense, fish can detect and distinguish the electrical properties of the close environment, measure distance, perceive the 3-D shape of objects and discriminate objects according to distance or size and shape, irrespective of conductivity, thus showing a degree of abstraction regarding the interpretation of sensory stimuli. The physical properties of images projected on the sensory surface by the fish's own discharge reveal a "Mexican hat" opposing centre-surround profile. It is likely that computation of the *image amplitude to slope ratio* is used to measure distance, while peak width and slope give measures of shape and contrast. Modelling has been used to explore how the images of multiple objects superimpose in a complex manner. While electric images are by nature distributed, or 'blurred', behavioural strategies orienting sensory surfaces and the neural architecture of sensory processing networks both contribute to resolving potential ambiguities. Rostral amplification is produced by current funnelling in the head and chin appendage regions, where high density electroreceptor distributions constitute foveal regions. Central magnification of electroreceptive pathways from these regions particularly favours the detection of capacitive properties intrinsic to potential living prey. Swimming movements alter the amplitude and contrast of pre-receptor object-images but image modulation is normalised by central gain-control mechanisms that maintain excitatory and inhibitory balance, removing the contrast-ambiguity introduced by self-motion in much the same way that contrast gain-control is achieved in vision.

Keywords Electrolocation · Electric images · Receptive fields · Sensory imaging · Modelling · Sensory magnification

J. Engelmann and J. Bacelo contributed equally to this study.

J. Engelmann (✉) · M. Metzen · R. Pusch · B. Bouton · G. von der Emde
Neuroethology and Sensory Ecology,
Institute of Zoology, University of Bonn,
Endenicher Allee 11-13, 43115 Bonn, Germany
e-mail: Jacob.Engelmann@uni-bonn.de

J. Bacelo · K. Grant
UNIC, CNRS, 1 Avenue de la Terrasse,
91190 Gif-sur Yvette, France

A. Caputi
Seccion Biomatematicas, Facultad de Ciencias,
Universidad de la República, Iguá 4225,
11400 Montevideo, Uruguay

A. Migliaro · R. Budelli
Departamento de Neurociencias Integrativas y Computacionales,
Universidad de la República, Av. Italia 3318,
11600 Montevideo, Uruguay

1 Introduction

The electric sense of Mormyrids is generally regarded as an adaptation to conditions less favourable for visual orientation. Although recent experiments show that the visual system is not as bad as expected in terms of resolution (Ciali et al. 1997; Wagner 2007), electroreception seems to be the dominant sense in orientation and communication tasks. When considering the role of the active electric system in electrolocation, however, it is essential to understand that conditions for the use of electric signal carriers in water are far from ideal, namely the good conductivity of water limits the range of detection of weakly electric fish to a few centimetres

(Heiligenberg 1977), depending on the object parameters. Nevertheless, given these limitations, electric fish exploit their electric sensory system to a degree that allows them to navigate and interact with their environment very well, independent of the visual sense. This is shown by the wealth of behaviours that are mediated by the electric sense, including foraging and prey detection, distinction between several objects, or location of other animals.

For the active sense that is under consideration here, the base for all these capabilities are the changes that are induced in the self-generated electric field by the presence of objects with a conductivity or capacitance that is different from that of the water. In analogy to the visual system, these changes, when projected onto the electrosensory surface, are referred to as the *electric image* of an object. Several studies have addressed certain aspects of electric images and the behaviours that rely on their reception (Budelli and Caputi 2000; Caputi and Budelli 2006; von der Emde 2006). However, we here present some behavioural examples that strengthen the idea that all sensory processing must be seen as an ongoing and hence "active" process, where neither sensory images nor exploratory behaviours are fixed. Instead, animals make use of the changes in their sensory world that for instance occur whenever there is relative motion between fish and objects, something we here refer to as the electrical flow (Egelhaaf et al. 2003; Karmeier et al. 2006). In contrast to visual flow, however, electric flow is less suitable for orientation in complex electrical environments because electric images are superposition images (Migliaro et al. 2005). This means that the electric images of objects, that in vision would occlude each other, can generate a combined electrical image without contours indicating overlap. Thus, multiple objects can fuse within an electrical image, making it difficult to extract contours or other features of individual objects (Caputi and Budelli 2006).

In the following, we address the question how the electrosensory world might be perceived by weakly electric fish. We focus on the pulse-type weakly electric fish *Gnathonemus petersii*, a member of the Mormyrid family found in Africa. We start by determining some passive properties of the electric field that must be taken into account and show how such passive properties might aid in active electrolocation. Based on the physical parameters of electric images, we address the physical constraints and discuss problems of electrolocation in *complex* electrical habitats, and we present some problems that are associated with movements of either the animal or the objects under inspection. Having elucidated the physical problems, we will relate them to both published and new behavioural data to determine cues that fish may use during electrolocation. Finally, we present new data on which aspects of an electric image are encoded at the level of the afferent nerve fibres and how the central representation of the electric world is organised in the brain.

2 Principles of electric images

The concept of an image is historically based on optical images because the optic apparatus of the eye is able to form a real image (real in the sense used in optics) on a surface by an imaging rule called central projection. Although the optical concept of a real image applies only to vision, the term image can be applied to any sensory system. In a generalized analysis valid for all sensory systems, Caputi and Budelli (2006) dissociated images into *the physical image* (the pattern of energy conveyed by pre-receptor structures), the *stimulus image* (the portion of the physical image that can be transduced by the array of sensory cells) and finally the *neural image* (the signal elicited by the stimulus image).

For example, *physical auditory images* can include infra- and ultrasound, whereas the *auditory stimulus image* only includes the range of frequencies to which the hair cells can respond. *Auditory neural images* would include the responses of the hair cells and afferents but also all other subsequent neural structures in the auditory pathway. Neural imaging generally implies the segregation of information. In the case of the auditory system, this segregation consists of a fast pathway that implements the Jeffress computational model (Jeffress 1948) for the determination of spatial parameters, and a slower pathway preserving frequency and phase of the sound to elaborate on the object properties.

The signals at the sensory surface are modulations of energy carriers. In electroreception the carrier constitutes the electric field that can also be expressed as current density. Two types of modulations are possible (Caputi and Budelli 2006): (1) modulations caused by changes in the characteristics of the carrier source or its position relative to the sensory surface; (2) modulations caused by the presence of objects that passively modify the field caused by the source. Stimulus images of objects generating the carrier are then defined as the effects of the carrier at the sensory surface. For electric images of objects that passively modify the field, the stimulus image is defined as the difference between the field including the object, and the field without the object. This then results in a new field that has been called as the object's "perturbing field" by Lissmann and Machin (1958). This field can be interpreted as being produced by the object's "equivalent source," which is directly related to a characteristic of the object referred to as "imprimence" by Lissmann and Machin (1958). The equivalent source is defined as the sources that would evoke a field identical to the perturbing field.

In the following, we apply the above framework to the analysis of active electric imaging. The electric image of a given object is the change in the transepidermal voltage due to the presence of an object. The simplest form of an electric image can be simulated by an electrical dipole which is equivalent to a small conductive sphere (Sicardi et al. 2000). The current density (J) at the skin is defined as

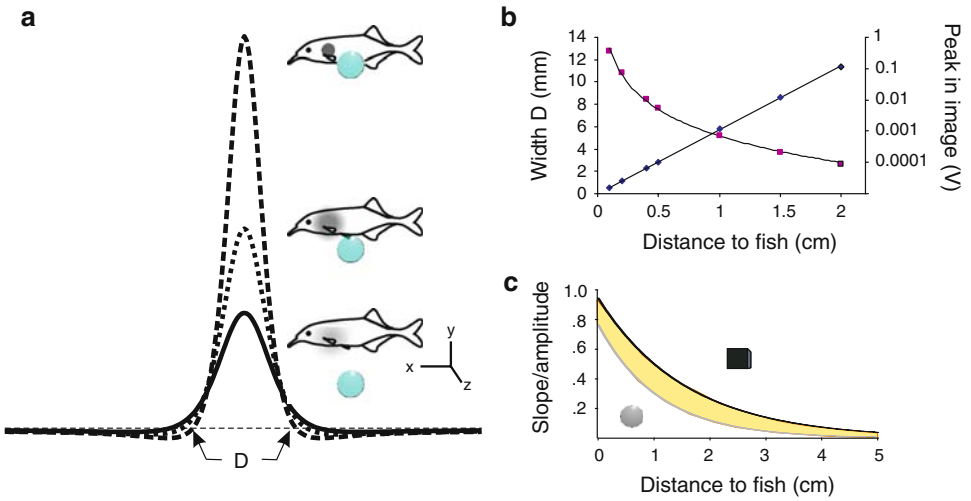

Fig. 1 Parameters of electric images **a** Spatial pattern of the transcutaneous current for a modelled dipole-like object (*small sphere*) at increasing distances as schematised by the fish. Note that the image increases in width but decreases in amplitude with distance. **b** Relation between width (measured as the distance *D* between the zero crossings indicated in **a**) and the amplitude of the electric image of a dipole as a function of the distance from the fish. **c** Maximum slope normalised to the maximal amplitude in the electric images of spheres (*grey line*) and cubes (*black line*) as a function of distance to the fish. Functions calculated according to von der Emde et al. (1998). Note that the normalised slope-amplitude ratios are different for a cube and a sphere, resulting in a horizontal shift of the slope/amplitude curve and giving rise to ambiguity in distance determination (highlighted by shading)

$$J_{n(x,y)} = \frac{\sigma_1 * \sigma_2}{2\pi\varepsilon_1(\sigma_1+\sigma_2)a^3}\left[\frac{p(x^2/d^2+y^2/d^2-2)}{x^2/d^2+y^2/d^2+1)^{5/2}}\right],$$

where σ is the conductivity, ε is electrical permissivity and d is the distance to the dipole. The principle properties of electric images can be illustrated well using such a dipole-field, which has the advantage of being easy to calculate. Figure 1 shows the current density profile (electric image) of such a dipole field for increasing distances from the skin. Several points should be noted. (1) Electric images differ from visual images in that a single point source in the electric world is projected on a two-dimensional surface in a centre/surround manner (*Mexican-hat* profile, Caputi et al. 1998). Hence, the physical image itself is blurred but this blur might be compensated by the contrast enhancing centre/surround structure of the electric image itself. (2) The blur, which is the width of an electric image, increases proportional to the distance and the amplitude of the images decreases proportional to d^2 (Fig. 1b). Although the data presented here are valid for a point source only, electric images of real objects differ from the described *Mexican-hat* profile only if objects are very close to the skin of the animal. (3) As amplitude and width of the electric image change with the distance to an object, they cannot be used as unequivocal cues for determining distances, since there is always ambiguity between object size and distance: a particular object might appear to be small because it is far away or simply because it is small. A way to disambiguate would be to calculate the ratio of the slope of the image to the maximal amplitude, a measure most likely used by the animals (see Sect. 3). Such a ratio resembles a normalisation of the electric image with respect to the peak amplitude, or, in other words, a normalised measure of the blur. While this parameter can explain several psychophysical results, fish can also be trained to distinguish different shapes, independently of the distance, or even to discriminate objects that only differ in their depth (see below). These capabilities cannot be explained based on the normalised slope alone, but rather depend on additional parameters that the fish must be able to extract from the electric image. This can be seen in Fig. 1c, where we plot the slope-amplitude ratio as a function of distance for spheres and cubes. This measure is independent of the size for spheres/cubes, but it does depend on the shape of the object, and fish can indeed be fooled to judge equally distant spheres and cubes to be at differing distances (von der Emde et al. 1998). The finding that they can learn to compensate for this ambiguity indicates that they must make use of additional cues. One possible solution to this problem might be contained in the dynamic cues the animal perceives while actively exploring the images and thereby changing its distance to the objects in a predictable manner.

A different solution to the distance discrimination problem has been proposed based on modelling work in the wave-type electric fish *Apteronotus leptorhynchus* (Babineau et al. 2006). Here it was shown that the width of electric images of objects can be a predictor of distance irrespective of object size and shape, for objects not too close to the animal. While

this works without a normalisation of the electric image, the behavioural data for *Gnathonemus* are in favour of the slope-amplitude measure. Additionally, the simpler model leaves fish with a different problem, which is that for larger objects the model would actually measure the distance to the centre of an object, but what most likely needs to be measured is the distance to the surface of the object. This can be resolved in principle by measuring the distance to the object's centre (image width) and subtracting the radius of the object. The latter parameter could be derived from the peak value in the electric image. However this would require some previous learning of the diameter/distance function. Also, the simpler algorithm applies only to modelled bimodal electric images (Babineau et al. 2006; Lewis and Maler 2001). These images are different form the *Mexican hat* -like images found in pulse-type electric fish (see Fig. 4 for an explanation of why electric images are *Mexican hat*-like). A third problem inherent to both proposed strategies is that the shape and therefore the cues extracted from electric images depend on the position of the object along the body axis. For example, the slope/amplitude ratio plotted in Fig. 1c is only valid at the trunk where the sensory surface is relatively flat, while for the head, where the sensory surface is quite strongly curved, an opposite picture is observed (Pusch et al. 2008).

Taking a comparative viewpoint it is remarkable that a similar mechanism for distance determination based on the width of sensory images has been proposed for the mechanosensory lateral line system (Ćurčić-Blake and van Netten 2006; Goulet et al. 2007). In this sensory system the distance to a hydrodynamic source can be determined based on the width of the hydrodynamic field in a manner similar to the mechanism proposed by Lewis and Maler (see above). This reflects the similarity of the physics in the two senses, however, behavioural data regarding the question whether fish make use of the proposed distance determination mechanism are still missing for the mechanosensory system.

2.1 Non-neuronal optimisations in electrolocation

Animals may modify the stimulus images that they receive in several ways and active electrolocation is a good paradigm for the study of such effects, since electric fish show alluringly simple examples of interaction with objects (Caputi 2004). (1) They generate the carrier (EOD) and set the coordinates of its source in such a way that the manoeuvre of approaching the tail of the fish to an object and moving it side to side may be useful for exploring large objects (Babineau et al. 2007). See Fig. 7a for an example of how a fish explores an object (see also additional online material). Fish may also control the reception of the image by pre-receptor conditioning of the signals for instance, in the way that the fish body funnels the current flow longitudinally, producing passive amplification of the signals at the peri-oral region. This is particularly important because an electrosensory fovea has been described in this region on the basis of electroreceptor organ density, variety and the enhanced central representation of these regions (Castelló et al. 2000; Migliaro et al. 2005). (3) Some fish, for example *G. petersii* have a moveable chin appendage, which serves as an additional fovea, allowing, the fish to actively explore objects (Pusch et al. 2008; von der Emde 2006). The similarity of the moveable fovea with regard to vision is discussed in detail below.

In mormyrids, the electric organ is relatively small and is restricted to the caudal peduncle (Lissmann 1958). The field produced by the basically biphasic EOD of *Gnathonemus* is an asymmetric dipole field with a smaller pole at the fish's tail and a larger pole constituting the entire body of the fish anterior to the electric organ. Several mechanisms and adaptations can be found that optimise the electric field for the task of electrolocation. The most important adaptation is the low internal resistance of the fish's body, as originally pointed out by Heiligenberg (Heiligenberg 1973), which enables the animal to generate a field over its whole body rather than the field being shunted at the tail. The low resistance together with the elongated shape of the fish accounts for a second mechanism termed "electric funnelling" (Castelló et al. 2000). This means that the voltage drop over the electroreceptors is maximized at the head and the tail, but is low orthogonal to the midline (Kalmijn 1974) (Fig. 2).

The above mechanisms all enhance the carrier properties for *electrically illuminating* objects near the nasal region and the chin appendage, were electrosensory foveas have been described (von der Emde 2006). In this most rostral region, both the signal carrier properties are optimised, and the electroreceptor densities are highest (Bacelo and Grant 2001; Harder et al. 1967; Quinet 1971).

According to this hypothesis, the head region should be used preferentially by the fish when extracting detailed information from surrounding objects. While direct behavioural data on this is currently lacking, the way objects cast their electric images on the head region corroborates the hypothesis: electric images of any object are symmetrical in the head region (see Figure 3b) and differ from those at the trunk, where images are skewed and their shapes depend on the rostro-caudal position of the object (Babineau et al. 2007). Hence, although the object causing the electric image may be symmetrical, images at the trunk are not. Furthermore, the electric image of a given object at the trunk depends on its relative position. The behavioural experiments that will be described below show that *Gnathonemus* is able to distinguish the shape of electric images even though these images are different, depending on whether they fall on the head or the trunk. Whether these differences give rise to ambiguities is currently unresolved.

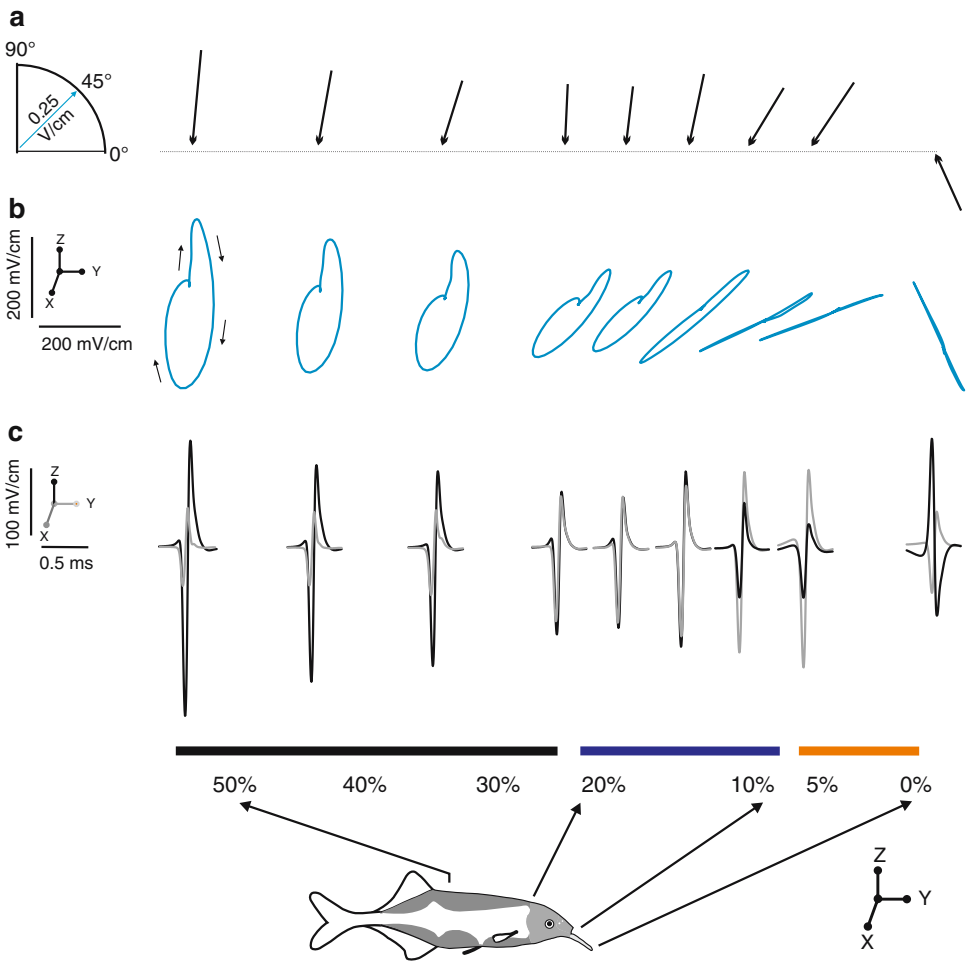

Fig. 2 Examples of several EOD parameters investigated along the length of a fish. The recording site is indicated relative to the long axis of the fish, shown as a percentage of whole body length, the mouth being zero. **a** Field vectors calculated at the time of the peak of the field module (not shown), i.e. the vectors represent the effective stimulus strength and direction. Vectors of 90° are oriented orthogonal to the sensory surface. **b** Trajectory of the field vector based on the *z* and *y* measurements of the local EODs. The direction of rotation of the vector loop is shown by the arrows on the left-most loop. Note that the *z* and *y* trajectories for the measurements made at the head are in phase but at the chin appendage they are 180° out of phase and show negative co-variance. **c** Examples of the *z* (*dark lines*) and *y* (*light lines*) local EODs. Again, the head and chin appendage stand out as regions where the *z* and *y* field components are exactly in phase and exactly 180° out of phase respectively, resulting in a stimulus direction of the field vectors (see a) towards the chin appendix. All data shown in this figure are averages of 15 consecutive measurements

One documented case where ambiguities arise during the interaction between the animal and the sensory world is that caused by body movements. These movements induce modulations in the electrical field and, in analogy to saccadic suppression in the visual system electric fish, it has been suggested that there may be specific mechanisms that might cancel these distortions that are due to such self-induced modulation of the electric field. In fact, movement of the chin appendage of *Gnathonemus* during foraging can reach velocities of up to 800°/EOD (Hollmann and von der Emde 2007). A sequence of such a saccade-like spontaneous Schnauzenorgan movement is available as additional online material. For this special case, however, our data show (Pusch et al. 2008) that the passive pre-receptor mechanisms help to resolve the ambiguities. When passively moving the chin, we have found that the field around the chin appendage is funnelled accordingly. It is the anatomy of this finger-like appendage that stabilises the electric field during the movement, due to the funnelling of current (Fig. 3a). In addition, this funnelling increases the illumination of an object that is inspected with the chin. Thus, the purely passive properties turn the chin appendage into a moveable searchlight for electrolocation. This is again in line with the idea of an electric fovea, since high resolution at a small part of the sensory surface should be accompanied by a mechanism to focus this fovea on a specific point of interest in the sensory world.

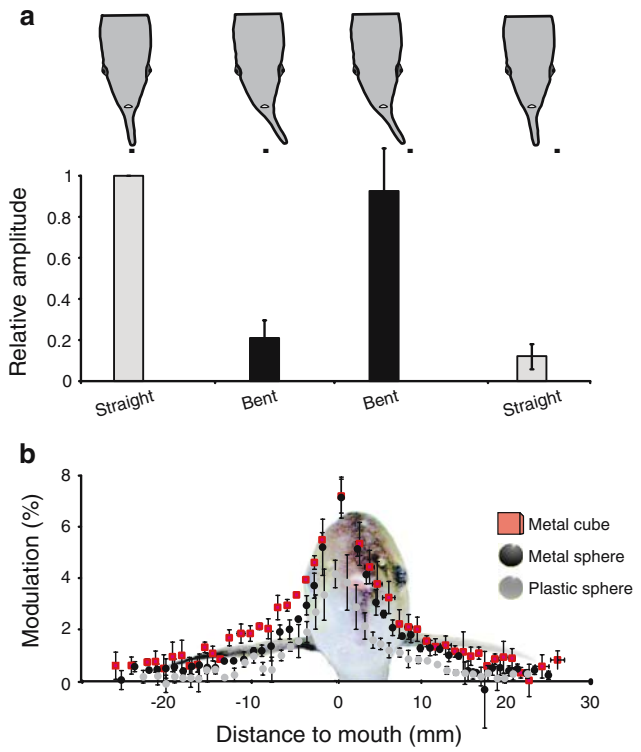

Fig. 3 **a** Effect of movements on the normalised amplitude of the electric field at the tip of the chin appendage. The diagram on the upper left shows the fish's head with a recording electrode (*blacksquare*) at the tip of the chin appendage. At this point, LEOD amplitude was maximal, as indicated in the histogram below. LEOD amplitude decreased by 80% when the chin appendage was bent laterally, mimicking natural saccadic scanning movements. Moving the recording electrode to the displaced tip of the chin appendage restored LEOD amplitude, but LEOD amplitude was again reduced if the chin appendage was returned to the straight position without following with the recording electrode (*top right*). **b** Mean ($n = 3$) electric images of a 2 cm radius metal sphere (*solid circles*), a 2-cm plastic sphere (*light circles*) and a 2×2 cm metal cube (*squares*) measured at the head of the animal. Note that images are symmetric and are similar in amplitude for the metal objects, although the sphere has the steeper slope. The image of the plastic sphere (*light circles*) has been flipped vertically to allow comparison of the difference in the shape of the image compared to that of the metal sphere. (Normally the presence of a plastic sphere would reduce LEOD amplitude and this would appear as a negative modulation curve). Water conductivity was $100\,\mu$S

2.1.1 *Effects of the fish body on electric images*

In order to understand the funnelling effect, modelling studies were employed to investigate how the fish body itself introduces a non-homogeneity in the media that surrounds the electric organ. Details of the models can be found in Caputi and Budelli (1995), Caputi et al. (1998) and Rother et al. (2003). We here present the basic assumptions of the model, based on the doctoral thesis of Diego Rother and some later changes to the software made by Heric Rodriguez (details available online; (Rother et al. 2003)).

The model is based on the following assumptions. All media are linear ohmic and isotropic. This means that the vector representing the current density at the point $x(J(x))$ is proportional to the vector electric field $(E(x))$. at the same point.

$$J(x) = \sigma(x).E(x), \quad \sigma(x) > 0.$$

The proportionality constant, $\sigma(x)$, referred to as "the volumetric conductivity at the point x" is always a positive scalar.

Capacitive elements are not included in the model. Therefore, there is no charge accumulation in any point of space. In mathematical terms, the variation of the density of charge $(\rho(x))$ is null.

$$\frac{\partial \rho(x)}{\partial t} = 0.$$

Given that the dielectric relaxation of the media is much smaller than the minimum period of the significant components of the EOD Fast Fourier transform, the model is an electrostatic approximation.

The fish and other objects are immersed in an infinite medium of water. The shape of the fish body and objects are approximated by an external surface composed by triangles, allowing an approximation of the object's shape as close as desired, limited only by the computational power available. The fish body, and any other object, may be covered by a thin resistive layer whose resistance may be introduced in the model and which may be different in different areas of this skin, as is the case for the fish body.

The model is based directly on the charge density equation which, in the context of our assumptions, implies that the charge generated by the sources $(f(x))$ is equal to the charge diffusion

$$\nabla J(x) = f(x) \Rightarrow \sigma.\nabla E(x) = f(x)$$

and therefore

$$\sigma.\nabla^2 \phi(x) = -f(x),$$

where $\phi(x)$ is the local potential at the point x. This differential equation, the so-called Poisson equation, can be solved using the boundary element method (Assad 1997). This method uses the given boundary conditions to fit boundary electric values (electric field and current density), and not the values throughout the whole space. From this, the electrical potentials can be calculated at any point in the surrounding water. This method determines the boundary electrical distributions solving a linear system of $2 \times N$ equations for N nodes, where the unknown variables are the transepithelial currents and potentials that correspond to each node.

Because the presence of the fish is a constant component, it is a common convention to define the electric image of an object as the difference in the transcutaneous pattern of

current density introduced by the presence of the object. Since the animal's body itself will interfere with the generation of the electric image, this effect is rather complex with both the fish body and the environment interacting reciprocally (Migliaro et al. 2005). However, neglecting the effects between the fish's body and objects will result in crude approximations to the real electric images. Therefore, we must also consider the role of the fish body in the generation of electric images. Its presence has several consequences:

1. The electric field of a dipole in a homogeneous medium differs from the electric field produced by a dipole located at the tail of the fish mainly at the rostral region of the body where the electrosensory foveas are located (Migliaro et al. 2005). This is due to the high conductivity of the internal tissue which offers a low resistance path along the fish's longitudinal axis, causing an increase in the current reaching the foveal regions. In addition, reduction of surface at the peri-oral region and in the chin appendage increases the local current density in these regions (Caputi et al. 1998).
2. The large gradient in conductivity at the skin causes a perpendicular orientation of the local field stimulating the electroreceptors (Fig. 2). Figure 4 illustrates the situation when the field illuminates objects in the close vicinity of the fish's body, showing a comparison of the electric image of an object when assuming that the internal conductivity of the body is equal to the conductivity of the water, and the image of the same object generated with the internal conductivity of the fish being much higher than that of the water (Migliaro et al. 2005). An important feature of the effect of having a high internal conductivity separated from the environment by weakly conductive skin is that the electric images are not biphasic but have a *Mexican-hat* profile. This argues once more against a distance determination mechanism in *Gnathonemus* that would be based on the width of electric images alone. This alternative and simpler approach for distance determination based only on the width of the electric images has so far only been shown to be adequate for biphasic electric images (Babineau et al. 2006, 2007).
3. Field deformations introduced by the fish's body are neither constant nor independent of normal movements. The chin appendage is used constantly for exploring and *manipulating* objects and its movements introduce large changes in the carrier in relation to objects (Fig. 3 and online material). Other exploratory behaviours are characterized by a "reverse" approach where the tail is directed towards the object and is moved from side to side. Thus, fish may use exploratory movements to modify the field in a goal-directed manner, manipulating the energy source for electrosensory stimulation rather like a *searchlight* for electrically *illuminating* nearby objects. On the other hand, tail movements occurring during swimming may introduce undesirable changes in the carrier and, thus, in the electric image of the objects. The effect of such tail movements on the electric image of an object close to the head are illustrated in Fig. 9 and 10 and are further explored in the physiology section of this paper.

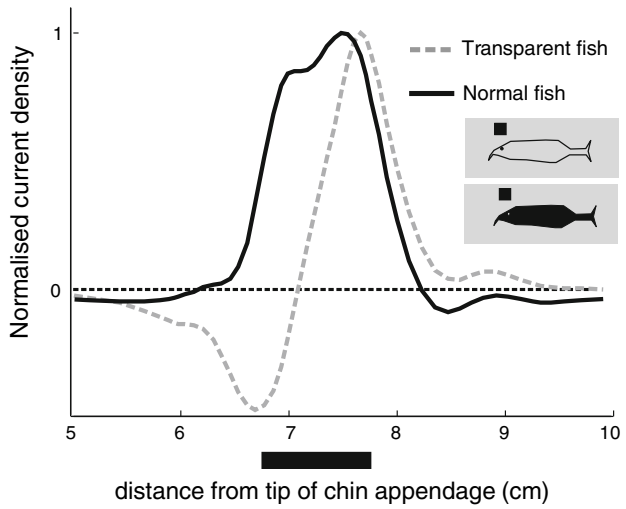

Fig. 4 Effect of the internal conductivity of the fish's body on the electric image. *Lines* show the transcutaneous current density modelled for a metal 1 × 1 cm cube. The position of the cube is indicated by the *black square*. The *grey line* represents the image when internal and external resistance are identical (see schematic at *top right*); the *black line* represents the image of the same object with a realistic (low) internal resistance of the fish's body. Note the *Mexican hat*-like shape of the electric image calculated for the realistically low internal conductivity of the animal

2.1.2 *Electric images in complex electrosensory scenes*

Up to now we have focussed on electric images of only one object. The stimulus image of a given object alone is simply the portion of its perturbing field that impinges on the sensory surface. However, this is a rather reduced situation since, especially in prey detection, animals need to discriminate their prey within a complex environment. Due to the nature of energy source, active electric images are superposition images. Thus, at each point of the electrosensory surface, the local stimulus is the sum of the basal carrier plus the effects of the secondary sources of the objects in the scene. Consequently, when two similar objects are placed some distance apart, the resulting image of these objects is close to the sum of the individual images (Fig. 5a). However, the resulting image may also be indistinguishable from other electric images of combined or individual objects (Budelli and Caputi 2000).

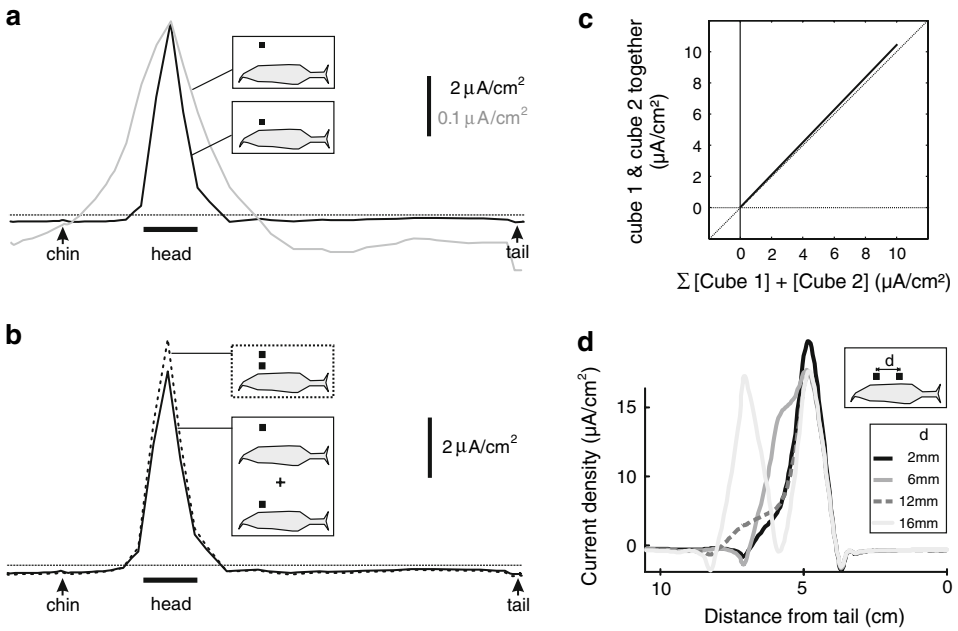

Fig. 5 Modelled electric images of metal objects. **a** Images of a 1×1 cm cube placed at two different distances from the skin: 0.5 cm (*black curve*) and 2.5 cm (*grey curve*). Note the difference in calibration. **b** Comparison of the calculated simple sum of the two individual images above (*black curve*) with the image obtained when both objects are present simultaneously in same positions as above (*dotted curved*). Note that the composite image produced by the two cubes present simultaneously is bigger than the calculated sum of the two individual images. **c** A plot of the amplitude of the composite images v. the calculated sum of pairs of individual images shows a curve with a slope >1. **d** The shape and amplitude of the composite image generated by two objects side-by-side depends on the distance (*d*) that separates them. Two separate images were discriminated when this separation was in the order of 16 mm

Since all objects immersed in an energy field are equivalent to new virtual sources, every object is both an emitting source and a receiver; therefore there are always multiple interactions when images of objects are formed in nature. A similar problem for vision, which is dealt with intuitively by painters, is that each object is illuminated not only by the main source of light, but also by reflections, and the reflections of reflections in the other objects of the scene. In electrolocation this has been called the object *perturbing field* (Lissmann and Machin 1958). Thus, when two objects are close to each other, the resulting image is different from the sum of the images generated by each object alone (Babineau et al. 2007; Pereira et al. 2005; Rother et al. 2003). This is shown in Fig. 5, where we moved a distant cube closer to the nearby cube. The interaction is sensitive to an increase in the distance between the objects, because the object perturbing field is much weaker compared to the initial field and therefore the interaction between objects decreases strongly with their distance. Similar data was obtained for non-conductive objects (not shown).

What has just been said about objects in apposition also applies to the superposition of individual objects. In this case, modelling data indicates that the minimal distance between two cubes which produce a composite electric image, still perceptible as two individual images, is in the range of 5–10 mm. Comparable data were obtained using relatively big objects by Rother for *Gnathonemus* (2003). Extending Rothers approach to smaller prey-like objects ($3 \times 3 \times 3$ mm) close to the animals' trunk (Fig. 5d) we confirm that small objects can be distinguished if they are not closer than 6 mm to each other. Using the inter-object distance that results in just measurable distinct peaks in the electric images as a measure of the minimal distance that objects must have in order to be perceived as separate objects (minimum separabilis), our results in *Gnathonemus* are strikingly similar to published data in *Apteronotus*. In *Apteronotus*, the minimum seperabilis under equivalent modelling conditions was found to be 4–9 mm (Babineau et al. 2007; Bastian 1981a,b).

It can be concluded that the rules of electric image generation can give rise to ambiguities for which the nervous system may have to compensate in order to use electric images to guide movements and cognitive behaviours. The relevant factors are (i) the funnelling effect introduced by the fish's body and its changes in shape during movements, (ii) the superposition rule inherent to the imaging process and (iii) the interaction of objects with the perturbing fields of other objects closely located.

3 Behaviour: which cues can fish detect?

Lissmann and Machin (1958) were the first to show that electric fish use active electrolocation in order to detect and

analyze objects in their environment. Active electrolocation in these fishes is based on the generation of a weak electric field that can be either a continuous sine-wave-like signal or a pulsed signal. Lissmann and Machin assumed that the fish detect only the electrical resistance of objects and consequently perceive a 'black-and-white' electrical picture of their surroundings. However, animate objects also have capacitive properties (Heiligenberg 1973), which lead to phase and waveform shifts of the local signal within the electric image. Mormyrids can detect EOD waveform distortions independently of EOD amplitude changes and thus can determine quantitatively the capacitance and the resistance of an object under investigation, i.e., they can determine impedances (von der Emde and Ronacher 1994).

Recently we showed that *Gnathonemus petersii* (Mormyridae) is able to perceive the three-dimensional shapes of objects independently of object distances. In these experiments, fish were trained in a two-alternative forced-choice procedure to discriminate between two differently shaped metal objects, e.g. a reinforced cylinder (S+) and a non-reinforced cube (S-) (von der Emde and Fetz 2007). When new object combinations were offered in non-rewarded test trials, fish preferred those objects that resembled their previous S+ and avoided objects resembling S-. For this decision, fish paid attention to the relative differences between the two objects they had to discriminate. The importance of shape in this task was demonstrated by reducing the objects to their three-dimensional contours, which sufficed for the fish to distinguish differently shaped objects. For object identification, fish attended mainly to the parameters volume, material, and shape, and to additional parameters, such as corners or rounded edges. When two unknown objects were offered, fish weighed positive and negative properties of these novel objects and based their decision on the outcome of this comparison.

A general question regarding these behavioural capabilities is to better understand whether the decisions are based on local features, or if objects are recognized as a whole. According to the hypothesis of feature extraction, the animal extracts and memorizes particular cues out of several possible ones that are present in the learned stimulus. As an alternative, fish would match the electric image that a novel object projects onto its electroreceptive skin surface to a stored template of the previously learned object. Then decision would depend on how alike a template and two offered alternatives are. Which mechanism fish use in this categorisation task is currently unknown, but the current data indicate that fish evaluate local cues to construct a representation of an object, which indicates a feature-extraction approach (von der Emde and Fetz 2007).

The presence of more than one object in close proximity to the animal generates complex electric images (see above). When an object is placed in front of a large background, the problem for the animal is similar to the figure-ground situation in vision and becomes additionally difficult due to the superposition character of individual images. Up to now, no experimental data on how fish perform under such conditions were available. To test whether fish can distinguish between shapes under these conditions, we trained fish to discriminate between a metal cube and a metal pyramid (S+). Following learning, test trials were conducted, during which a plastic or metal panel of $13 \times 13 \times 0.1$ cm was placed at various distances behind each of the two objects. These panels served as "backgrounds" in front of which fish had to differentiate the two previously learned shapes. Surprisingly, fish had no difficulties in discrimination even when the background panels were touching the objects (Fig. 6a). Shape recognition was perfect, no matter whether metal or plastic objects were used and when the objects were paired with metal or plastic backgrounds.

These findings show two interesting properties of shape recognition in *G. petersii*: (1) when trained to choose a metal object of a certain shape, fish also recognize plastic objects of the same shape. This is not trivial, since a plastic object casts an entirely different electric image onto the fish's skin, which is not just a mirror image of a metal object of the same shape (compare the rectified images of a metal/plastic sphere in Fig. 3b). (2) Regardless of the superposition of the object's and the background's electric images, no masking due to the background occurred. This might be useful for the fish, e.g. during foraging, when small worms or other prey items have to be found on the floor of the river in which they live. How the fish separate the electric images of the background and the object is unclear, but modelling work suggests that relative motion might be an important cue in such tasks as it will lead to temporal and spatial correlations in the electric images which will allow animals to distinguish small objects form larger backgrounds. Large objects in the environment will produce large, blurred images that will not change when the animal is moving, whereas the electric images of smaller objects (prey) nearby will change to a stronger degree (Babineau et al. 2007; Chen et al. 2005), leaving an "electrical signature" (electric flow) that animals could detect.

3.1 Distance determination

Fish are able to extract various parameters from electric images. One parameter of utmost importance is the ability to localise an object in 3-dimensional space. The simplest parameter the animal must extract to precisely localise an object is its position (x and y coordinates). As is shown in Fig. 1a, this parameter should be easily accessible for the animals, by simply determining the maximum amplitude in the electric image. However, determination of distance (z-coordinate) turns out to be less straightforward.

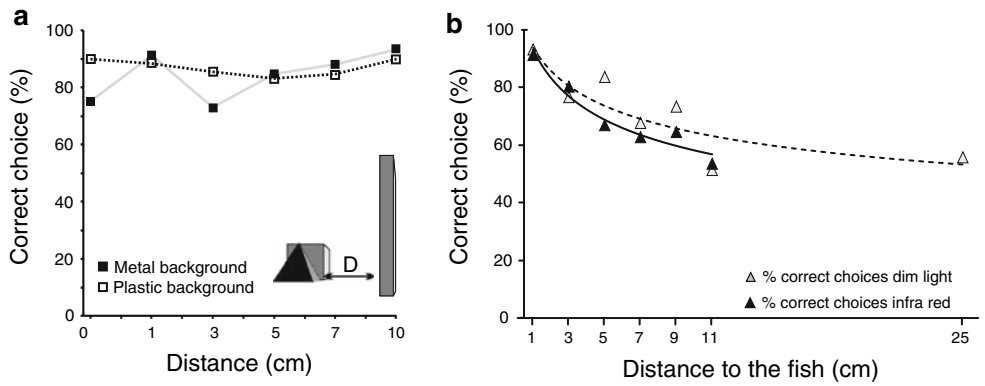

Fig. 6 **a** Discrimination performance of a fish trained to distinguish a metal cube (S−) from a metal pyramid (S+; both 3 × 3 × 3 cm), when the objects were placed in front of a metal (*solid symbols*) or a plastic background (*open symbols*) at defined distance (D). **b** Performance of the same fish, when the objects where placed at increasing distances from the animal (*without background*). *Grey symbols* indicate measurements obtained with dim illumination and *black symbols* indicate data obtained under infrared illumination which is invisible to the fish. Beyond 7 cm performance fell to chance level ($\chi^2 > 0.05$). Note that, as shown in Fig. 6b, performance was independent of background illumination

It is important to note that electric images are fundamentally different from optical images that are projected onto the retina of a vertebrate eye during vision. Because there are not any focusing mechanisms, electrical images are out of focus. They would be in focus only if the distance between object and skin is zero. Compared to an optical projection of a 3-D object onto a 2-D surface, electrical images are distributed or distorted. Optical images are determined by object shape, size, and other geometrical parameters. In contrast, electric images depend on several additional object properties, such as object depth, object distance, location along the fish's body and the properties of neighbouring objects. In vision, object distance can be deduced from binocular cues (stereopsis) and from other geometrical relationships within the retinal image. In the retinal image, geometrical relationships of the outside world are preserved because of the focusing action of the eye. As just mentioned, this is not the case for electric images, and therefore the ability to determine an object's distance based on its electric image is not a simple task. Several possible strategies could be used by fish, including measuring the half-width of electric images (which is only valid for point sources or objects of known size) (Lewis and Maler 2001; Rasnow 1996; von der Emde et al. 1998), or dynamic cues based on the electrical flow as explained above.

In behavioural experiments, *G. petersii* learned to distinguish which of two presented objects was located farther away than the alternative one: this was possible irrespective of size and electrical conductivity of the object's material (Schwarz and von der Emde 2001; von der Emde et al. 1998). In these experiments, the two objects were presented far away from each other, so that the fish could only examine one object at a time. As explained above, several different ideas exist on how this task is solved in electrolocation. For the above experiments with *G. petersii* the slope/amplitude ratio is the most likely candidate. This was shown by training fish to discriminate spheres and cubes, which differ in the slope/amplitude ratio due to their shape. When the objects were placed such that the ratios were identical, the animals confused the objects (Schwarz and von der Emde 2001; von der Emde et al. 1998).

3.1.1 How far away can the fish detect an object during active electrolocation?

As a rule of thumb, one can say that the distance over which a fish can detect medium sized objects in the cm-range, in water of natural conductivity (< 100 µS/cm), is a little less than one standard length of the fish (Schwarz and von der Emde 2001). The short range of electroreception is, at least to a certain extent, a consequence of the lack of focus of the electric images. This is similar to orientation with the mechanosensory lateral line (Goulet et al. 2007). In both senses, the notion of being a "near-field sense" is partially explained by the broadening of images with distance. Thus, big or far away objects will cast incomplete electric/hydrodynamic images on an animal. As a complete image is needed to correctly determine object properties, incomplete images of far-away objects can not be interpreted correctly by the fish.

If, in addition to simple distance determination, an additional analysis of the objects is required, the range over which this is possible is even shorter. For example, when *G. petersii* was asked to discriminate between objects of different shapes, such as between a pyramid and a cube (3 × 3 × 3 cm), discrimination performance broke down at about 5 cm from the fish (Fig. 6b). This performance was only slightly improved when lights were on. So, being able to use their eyes did not significantly help the fish to solve the problem, despite the finding that *G. petersii* can also learn

to visually discriminate between differently shaped objects (Landsberger and von der Emde 2007; Schuster and Amtsfeld 2002).

3.1.2 *Do fish determine the relative size of an object irrespective of the blur?*

In vision, an object is still recognized as being of a certain size no matter from what distance it is viewed (Douglas et al., 1988; Leibowitz 1971). The question as to whether such *size constancy* is present in electrolocation has not been investigated. We thus tested whether this also applies to active electrolocation where the width of electric images is a function of both size and distance. *G. petersii* were trained to discriminate between two differently sized cubes, one having a side length of 2 cm (S+) and the other of 3 cm (S−). During training, the fish learned to choose the smaller cube, which was placed at a distance of 1 cm from the fish, and to avoid the larger cube, which was placed at a distance of 2 cm. Following learning, unrewarded test trails with different object distances were conducted. Fish chose the small object no matter if it was closer to the fish, at the same distance, or further away than the large object (Fig. 7b). Performance did decrease with increasing distance for the tests where both objects were at the same distance (Logistic regression, Wald. 8.75, $P = 0.033$), but was not altered significantly in those cases where the relative distance between the objects was changed in addition (Logistic regression, $P \geq 0.1$). If object distance was increased to 4 cm, the fish could no longer identify the smaller cube, indicating that size constancy only exists close to the fish.

Similar to our results on shape detection, the identification of the smaller object depended on the volumes of the objects offered. This was shown training a second fish to choose between two cubes off different sizes, one $3 \times 3 \times 3$ cm and the other $2 \times 2 \times 2$ cm. When, following the learning, the original S− (large cube, $3 \times 3 \times 3$ cm) was replaced with an object that had the same frontal area but a smaller depth ($3 \times 3 \times 1$ cm) and this new object was presented together with the original S+ (small cube, $2 \times 2 \times 2$ cm), the fish could no longer discriminate between the objects. Even though the new object pair had the same silhouettes (3×3 cm and 2×2 cm) as the original pair used for training, the electric image of the new, flatter, plate-object was different from that of the original large cube. The smaller volume of the plate-object must have altered its electric image in such a way that it was no longer perceived as having a larger size than the small cube. This shows that we have to be very careful when comparing active electrolocation to vision, because other rules apply and other object parameters influence the electrical image on the fish's skin as compared to the visual image projected onto the retina during vision.

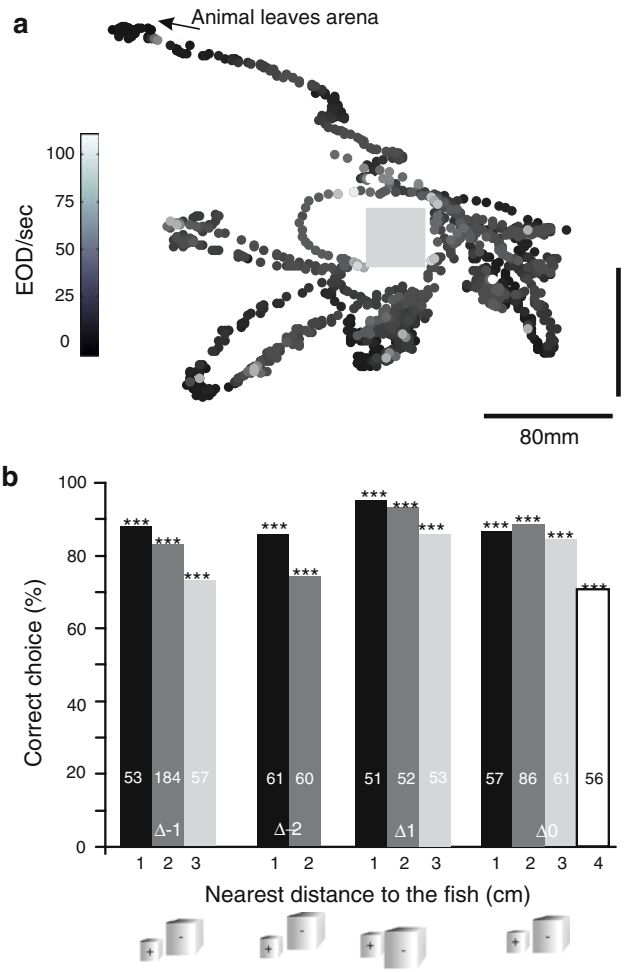

Fig. 7 **a** Tracking data of a fish exploring a $4 \times 4 \times 4$ cm plastic cube. Each *dot* represents the position of the animal (centre of gravity) at the time it emitted an EOD. The EOD-frequency is represented by the grey-scale of the individual dots (range 3–73 Hz). The sequence shown had a duration of 77 s with a mean EOD-frequency of 16 EODs/s. Note the increased frequency in the proximity of the object, especially the corners. A movie of the data shown here can be accessed online. **b** Performance of discriminating between small ($2 \times 2 \times 2$ cm, S+) and large ($3 \times 3 \times 3$ cm, S−) metal cubes. The percentage of correctly choosing S+ is shown ordered by the tasks the fish had to perform. The distances on the *X*-axis refer to the closest distance to an object in these tasks. From *left to right*: initial training with S+ being 1 cm closer to the fish than S− (Δ-1); in the following task the distance between S+ and S− was increased to 2 cm (Δ-2). In the third task the initial training condition was reversed, i.e., S− now was closer to the fish (Δ + 1). Finally both objects were presented at the same distances (Δ0). In all cases (number of trials is shown by the numbers in the columns) fish successfully distinguished S+ and S– (χ^2 test: *** P <0.0001), but discrimination decreased with increasing distance

4 Neuronal coding of electric images

4.1 Conversion of the physical stimulus in a neuronal code

Extending the above data to the neural coding of sensory images, our initial question is, *which aspects of the electric*

image are encoded in electrosensory neural activity? As pointed out above, electric images are caused by the presence of nearby objects that differ either in their resistance or capacitance from the surrounding water. In the active electric sense of Mormyrids these two aspects of the sensory world are processed by separate types of sensory cells within each electroreceptor organ (type A and type B cells in mormyromasts). Here, we consider only those receptor cells that are concerned with the analysis of the resistive (amplitude) properties of electric images, the so-called A-cells of the mormyromasts.

Since the initial work of Szabo and Hagiwara (1967) it has been known that mormyromast primary afferent fibres discharge a burst of several spikes to the fish's own EOD and that the latency and rate within the burst depends on the EOD-amplitude. In the following section we describe how electric images of single conductive objects are perceived by the mormyromast A-cells primary afferents.

Briefly, a $6 \times 6 \times 6$ mm metal cube was passed in a stepwise manner through the receptive field of recorded mormyromast afferents, and spiking activity was recorded in the medial zone of the electrosensory lobe (ELL) simultaneously with the local electric field (LEOD) generated by the object at the electroreceptive skin surface. The LEOD was recorded between a platinum electrode placed as close as possible to the skin and an indifferent electrode inserted in the back muscle. The recording electrode was placed at the centre of the receptive field of the recorded primary afferent fibre. In this experimental paradigm, the recorded electric image of the object is the convolution of the asymmetrical Mexican hat profile of the electric image with the basal LEOD at the point of the recording electrode (see Fig 3 in Gomez et al. 2004).

Of the ten primary afferents recorded in the deep layers of the medial zone of the electrosensory lateral line lobe (ELL), nine afferents fired three action potentials in response to the natural EOD without an object present, while one afferent fibre fired only two action potentials. The response latency was a function of LEOD amplitude at the centre of the receptive fields. Although only weak modulations of the basal EOD amplitude were evoked by the object (2–6%), the primary afferent fibres clearly responded to these small modulations by a change in spike latency (Fig. 8). The latency of all spikes was shortest when the LEOD amplitude was greatest (Fig. 8) while the number of spikes/EOD was constant. Previous studies have illustrated changes in the number of action potentials with stimulus intensity when using an artificial dipole stimulus and a much larger range of stimulus amplitudes, which were possibly, at least partially, outside the physiological range (Bell 1990; Szabo and Hagiwara 1967).

The timing of the first spike of the primary afferent response was very precise for any given position of the object (Fig. 8d), but the variability of spike timing was greater for the second and third spikes. In the example illustrated, the mean precision of the first spike was 19 μs with a range of variation of 233μs. Latency variability increased for the second and third spikes (Fig. 8e, f), however, and the mean precision found for the population of primary afferents was $33 \pm 27\mu$s ($N = 8$). Figure 8d–i shows a more detailed analysis of the coding of stimulus intensity in the primary afferent response. The spatial tuning curves for each spike in the burst response were expressed as mean $\pm$ standard deviations of the spike latencies for each object position. The spatial tuning curves of Fig. 8d–f are not symmetrical around the centre of the receptive field (Fig. 8d–f). This is because the Mexican hat profile of the physical stimulus is itself asymmetric, with a deeper trough on the rostral front due to the caudal location of the energy source (Caputi et al. 1998; von der Emde et al. 1998).

Within the range of LEOD amplitude modulations that our small object evoked, we found a linear relationship between stimulus amplitude and spike latency. In the example of Fig. 8, the linear regression accounts for 91% of the total variance observed in the latencies of the first spike (Fig. 8g). Although the linear regressions for the other spikes have steeper slopes, they also present an increased total variance, such that they do not add any more information related to the LEOD amplitude than that which is already transmitted by the first spike latency.

We conclude that for the encoding of electric images by the afferents, the timing of spikes is the most important parameter. Our data show that the latency changes that are induced by the electric images of objects, which are big compared to prey items, are in the sub-millisecond range. Changes in the electric images induced by typical prey may be too subtle to alter spike latency or firing rate at the primary afferent level even to this extent. This means that central neurones will have to resolve minute differences in timing information. It also explains in part why corollary discharge mechanisms are prominent in the brain of these fishes since such a mechanism enables the animals to reliably compute timing differences relative to the EOD which is a fixed reference point. An additional problem, not considered here, that probably needs to be taken into account, is the recent finding that the latency-code of the afferents is highly variable (Sawtell et al. 2006) and does depend on the previous EOD-discharge frequency.

4.1.1 Ambiguities due to motion

When discussing the pre-receptor mechanisms we pointed out that motion can give rise to ambiguities in electric images. This has not yet been investigated in Mormyrid fish. Thus, we investigated the influence of fictive swimming. As the tail moves from side to side, this results in changes in the geometric structure of the electric field and alters the distance of the electric organ from the sensory surface. Sudden jumps in the

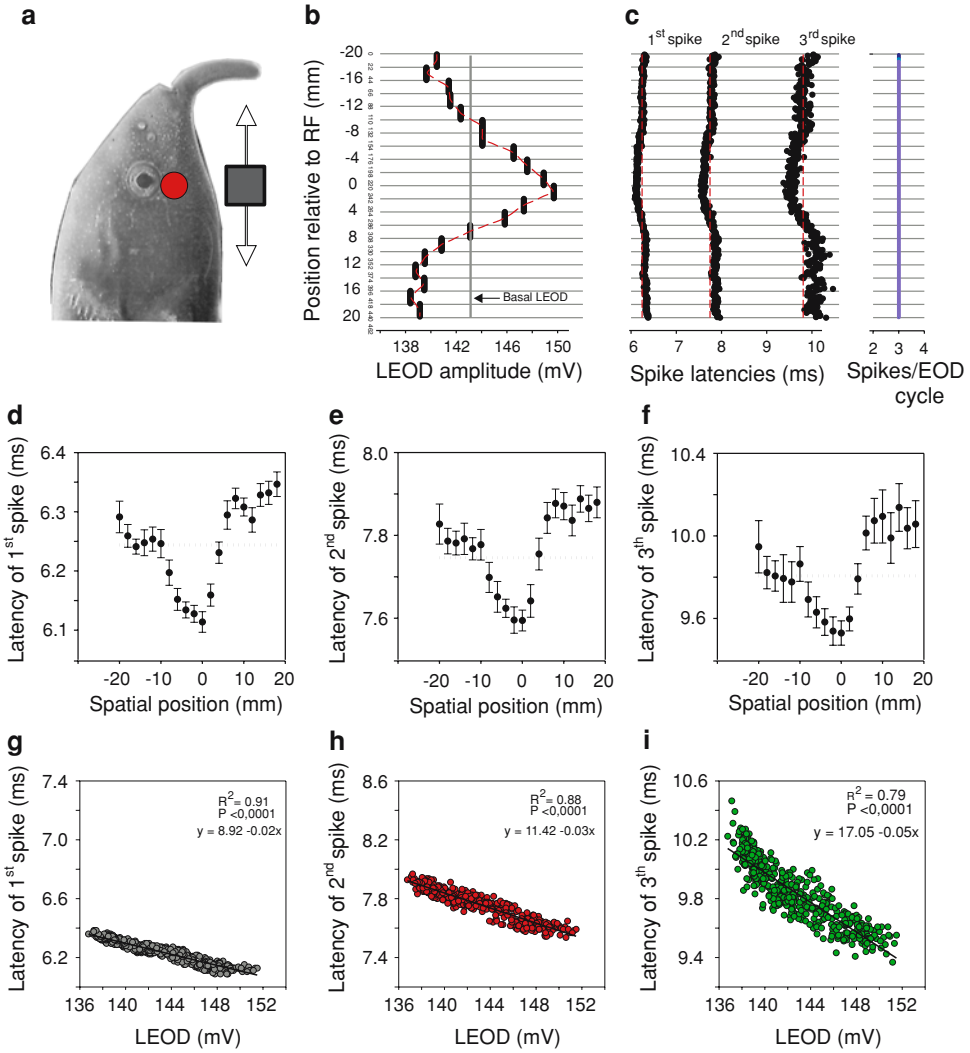

Fig. 8 Receptive field and electric image coded by a primary afferent. **a** Side view of the head of the fish with the location of the innervated mormyromasts shown by *red circle*. The *grey arrows* indicate the relative movement of the metal cube. **b** Amplitude of the local EOD measured at the centre of the receptive field while moving the object laterally through the receptive field. At each position ten successive EODs were recorded (see *y*-axis for position of object). The *vertical line* represents the basal EOD amplitude in the absence of the object, measured at the centre of the receptive field. **c** Raster plot showing the timing of the primary afferent spikes recorded at each position and the absolute number of spikes per EOD (*far right*). **d–f** Mean latencies of the first (**d**), second (**e**) and third (**f**) spike as a function of object position (referred to as receptive field plot; 0 = centre of receptive field). **g–i** Spike latency of first (**g**), second (**h**) and third (**i**) spikes as a function of local EOD amplitude

EOD intensity might therefore be expected. Electric images on one side of the fish will be of overall higher intensity when the fish discharges the EOD with the tail bent towards that sensory surface, compared with when the tail is straight. The opposite would be expected when the tail is bent contralaterally (Fig. 9).

Such movements do indeed have a considerable effect on the timing of primary afferent spiking (Fig. 9). Here we measured the response of a primary afferent during fictive swimming. Motion was comparable to the natural swimming movements and the changes in EOD-amplitude associated with this motion are reflected in changes of the latency of the spiking-response to the EOD.

This body-movement-induced change in the basal EOD amplitude will produce an ambiguity in the electric image as it is conveyed by the primary afferents. Consequently, the image of a given object will depend on the instantaneous position of the electric organ. We therefore investigated to what extend such ambiguities are contained in the primary afferent firing pattern. Figure 11a shows the electric images of the same metal cube for two conditions: with the fish's tail maintained straight (black curve) and with the tail bent 22° ipsilaterally (red curve). When the tail is bent ipsilaterally, the electric organ is closer to the receptive surface on that side and overall stimulus intensities, measured as the LEOD peak-to-peak amplitude, are increased by about 8%. This change is almost as big as the modulation caused by the presence of the conducting object itself. However, when the electric images of the object obtained at each body position are plotted as the modulation of the basal LEOD at that same position, the form and degree of modulation are comparable when the tail is bent or straight (about 10% in this example; 5–10% in the whole population of recorded afferents) (Fig. 11d). A second, qualitative change in the electric image profile can also be observed in that the negative trough of the Mexican hat is slightly enhanced when the tail is bent.

The differences in electric images are reflected in the neuronal responses of afferents. Figure 11b shows the spatial

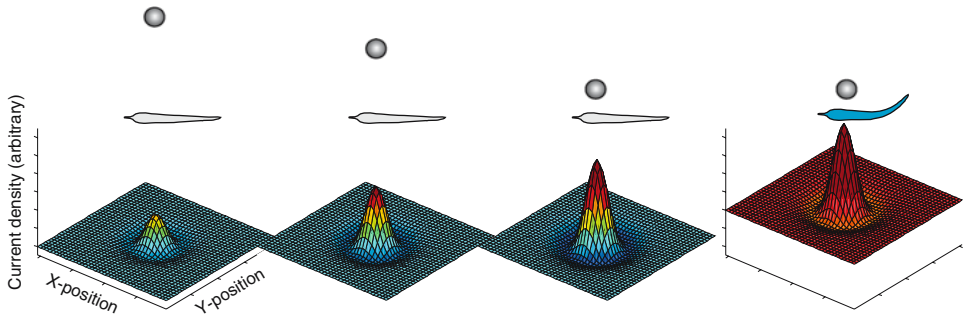

Fig. 9 Schematic representation of the electric images, indicated in a colour-code with brighter colours representing higher intensities of the image, projected on the skin of the fish by a conductive sphere decreasing in distance (*left* to *right*). The plot on the far right shows the effect of bending the tail towards the sphere: this increases the basal LEOD amplitude (illumination) but decreases the contrast between the image and the basal LEOD

profile of the neuronal response of the afferents to the electric images in the two body positions. Here the receptive fields were mapped statically, using passive bending of the tail rather than active swimming movement. The higher intensity of the LEODs in the tail-bent condition evoked primary afferent responses with shorter latencies than those obtained when the electric organ was perfectly aligned with the body. Right at the centre of the electric image, the precision was slightly higher in the tail-bent condition for this primary afferent (24 μs vs. 14 μs). The range of latencies used to encode the electric image of the object was also significantly different in the two situations. When the tail was bent, the range of latencies — from shortest to longest - was only half that of the range occurring in the straight position. This is due to the hyperbolic relationship between stimulus intensity and primary afferent spike latency, originally described by (Szabo and Hagiwara 1967). Figure 11c shows a plot of first spike latency versus LEOD amplitude grouping data for both "tail straight" and "tail bent", illustrating this hyperbolic relationship. Local EOD amplitudes observed when the tail was bent fall in the part of the curve where the slope is less steep and thus, although stimulus intensities were actually greater, the image projected was in fact flatter compared to the situation when the tail was straight. This is comparable to a reduction of contrast in the visual domain and it is important to understand that such changes in electric contrast will be encountered continually during normal active swimming, where each EOD will produce a snapshot that will encode the electric image on a different region of the hyperbolic function, leading to continual shifts in the range of latencies used to encode the electric image of the object.

While we have demonstrated that the absolute physical properties of electric images are reliably conveyed in the form of a latency code by the electrosensory primary afferents, our data indicate that central neurones will have to resolve the contrast-ambiguities in order to extract unambiguous information. We suggest that these ambiguities are resolved in the ELL by a gain-control mechanism by which, at the same time that an excitatory response is recorded in some neurones, sensory input also regulates the activity of local GABAergic inhibitory interneurones such that the effects of the given sensory input are normalised with respect to the basal LEOD amplitude. This will remove the contrast-ambiguity in the electric image (c.f. Fig. 11d) at the output-level of the ELL. (An article is in preparation on this subject.) The proposed mechanism differs from data published for Gymnotid fish where the effects of tail bending were shown to be cancelled out within the ELL based on adaptive mechanisms (Bastian 1995). The advantage of the proposed gain-controlled mechanism is that it does not depend on predictive or sensory signals apart from the electric information available at the periphery at the time the image is obtained. Adaptation however depends on additional electrosensory and/or proprioceptive input, working on a longer timescale.

Behavioural support for a mechanism that resolves the contrast-ambiguity comes from a recent studies in *Gymnotus* (Pereira et al. 2005) that showed that these fish respond to the change within electric images. This indicates that the behavioural response to an electric image depends only on the departure of each new image from a baseline image, stored in the brain of the fish and resulting from the integration of previous images.

This would strengthen the need for either central adaptation or a gain-control mechanism in order for the fish to be able to evaluate the changes in the environment with respect to the momentary basal electric field, removing the contrast-ambiguity introduced by the self-motion (Figure 10). In fact, the neural mechanisms for such a kind of computation have been described in mormyrids (Bell 1981; Bell et al. 1997b, on the ELL, Bell and von der Emde on praeminentialis). However, fast movements, for instance the tail bending of pulse mormyrids during swimming, need to be compensated by a mechanism fast enough to match the signal variability. Therefore, we suggest that ambiguities created by fast movements are resolved in the ELL by a feed forward, gain-control mechanism by which, at the same time that an

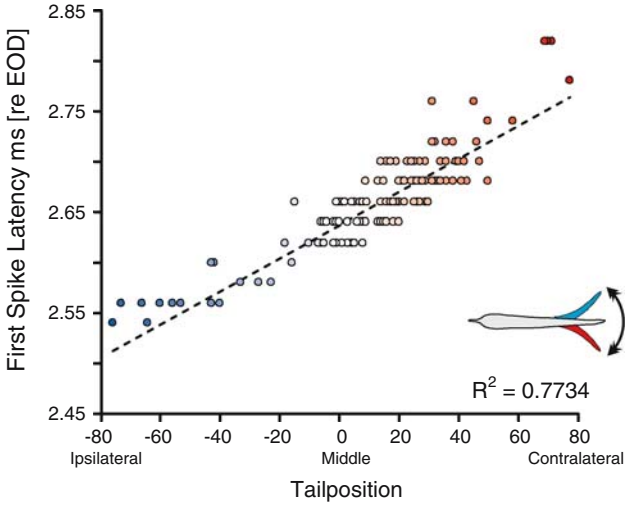

Fig. 10 Effect of natural swimming on the first-spike latency recorded from a primary afferent innervating a mormyromast type A-cell with a receptive field on the left side of the fish. Latency is plotted as a function of tail position, with position being depicted as the pixel displacement of the tail measured from a digitized photo image. The maximum displacement was ±12° in this recording

excitatory response is recorded in some neurones, sensory input also regulates the activity of local GABAergic inhibitory interneurones such that the effects of the given sensory input are normalised with respect to the basal LEOD amplitude. This will remove the contrast-ambiguity in the electric image (c.f. Figs. 9, 11) at the output-level of the ELL. (An article is in preparation on this subject.)

The proposed mechanism differs from data published for Gymnotid fish where the effects of tail bending were shown to be cancelled out within the ELL based either on feed back gain control or on adaptive mechanisms (Bastian 1995). The advantage of the proposed gain-controlled mechanism is that it does not depend on predictive or sensory signals apart from the electric information available at the periphery. Adaptation, however, depends on additional electrosensory and/or proprioceptive input.

4.2 Central representation of the periphery

We now turn to the question of how electric images are represented at the first central processing station, the

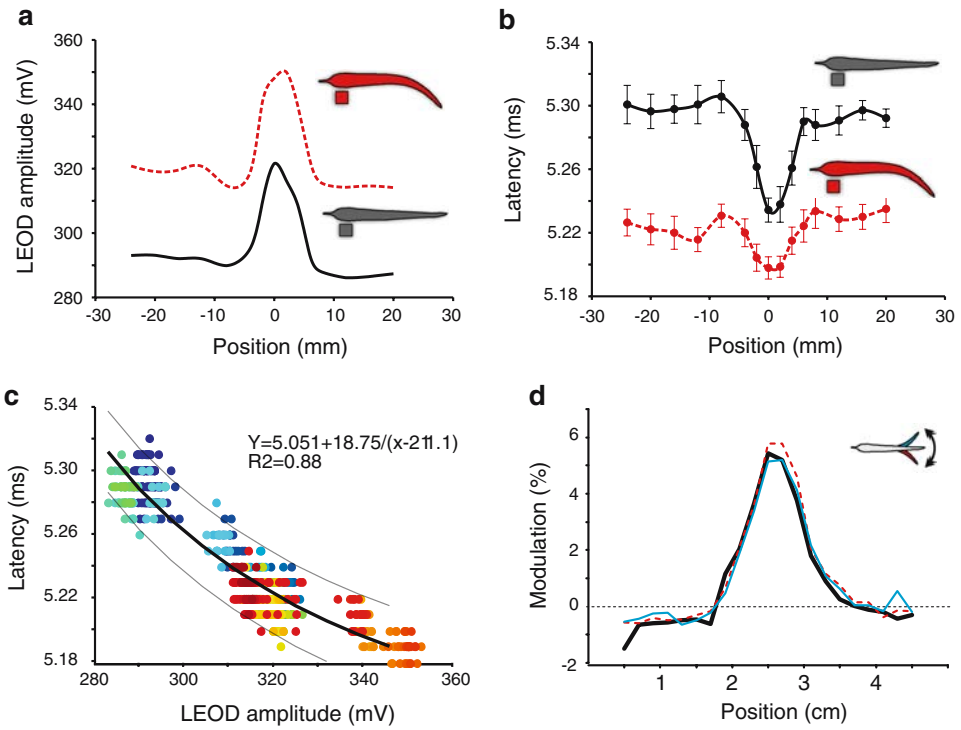

Fig. 11 Effect of a passive tail-bend on the electric image (**a**, **d**) and the response of a primary afferent (**b**, **c**). **a** Electric image of a metal cube measured as the peak-to-peak LEOD amplitude, with the tail straight (*solid curve*) and bent (*stippled curve*); the distance of the object remained unchanged. Note the overall upward shift in the image amplitude range when the tail is bent towards the object. **b** Receptive field of a primary afferent plotted as the first spike latency versus the spatial position of the object for the two electric images shown in **a**. **c** The latency of all spikes recorded with the tail straight and bent, as a function of the local EOD amplitude. *Red* to *yellow* colours mark latencies measured with the tail bent ipsilaterally; *green* to *blue* colours refer to the straight condition. Note that while data with the tail either straight or bent are best fit by a linear regression, when all data are pooled, the best fit is a hyperbolic function. **d** Normalised electric images of the same object used in **a–c** but measured separately while the tail was displaced to the ipsilateral (*stippled line*) and contralateral (*thin solid line*) sides. Note that the normalised images are almost identical. The *black thick curve* shows the LEOD profile in the basal condition, with the tail straight and in the absence of any object

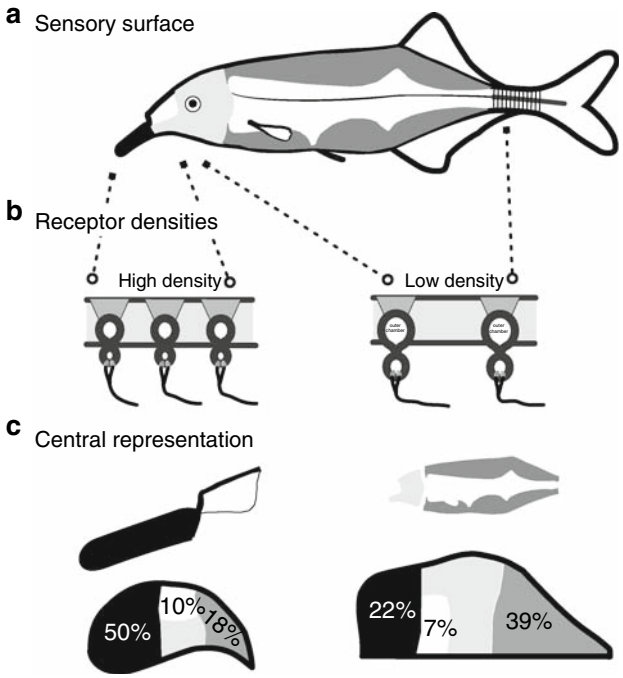

Fig. 12 Schematic representation of the peripheral and central representation of the afferents innervating mormyromast A-cells (sensitive to the amplitude of the EOD) and B-cells (sensitive to the waveform of EOD) in the ELL as revealed by tracing experiments. **a** Schematic showing the different body zones, of which the head and chin appendage correspond to the "foveal regions". **b** Schematic showing the receptor densities in the different regions. **c** Corresponding representation of these regions in the brain drawn to scale (*top*) and a flat-mount view of the dorso-lateral (*left*) and dorso-medial (*right*) zones of the ELL showing the relative distributions of the projection from the B-cells and A-cells respectively, for the body zones designated in a. This illustrates the central relative "over-representation" of the chin appendage and nasal region

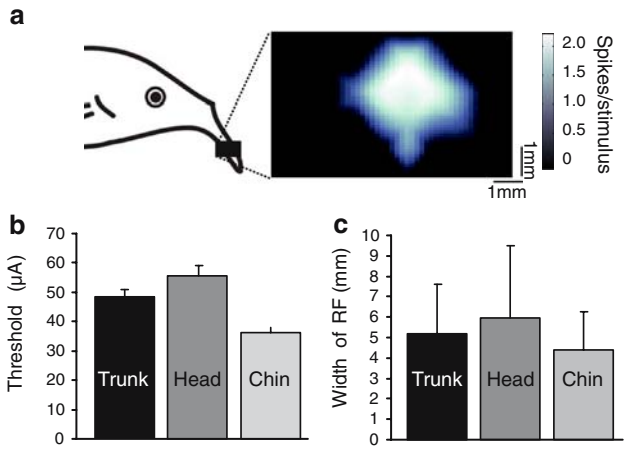

Fig. 13 Organisation and size of primary afferent receptive fields. **a** Receptive field of an mormyromasts recorded at the chin appendage (*left side*). The receptive field was mapped in 2 dimensions and is plotted at the right side using a grey-scale for the mean rate obtained at each position. **b** Comparison of thresholds in afferents with receptive fields on the chin appendage and on the head. Threshold was determined as the amplitude of a local dipole constant current stimulus required to evoke spiking in the afferents. **c** The mean maximum width of recorded receptive fields, recorded as in b)

electrosensory lateral-line lobe (ELL) situated immediately ventral to the cerebellum in the rhombencephalon. Anatomical data shows that the foveal regions are subjected to a central magnification (see Fig. 12), i.e., the area of the ELL devoted to the processing of input from these regions is disproportionally greater than the representation of the rest of the body. This finding supporting the presence of a foveal region is similar to that described for pulse Gymnotids (Castelló et al., 1998) and is comparable to the representation of the fovea in the visual cortex (Azzopardi and Cowey 1993) or of the 11th star in the somatosensory cortex of the star-nosed mole (Catania 1999), where such "cortical" magnifications have been associated with improved spatial resolutions.

In order to better understand how the different sensitivity and spatial resolution of different body regions are represented in the central electrosensory network, the receptive fields of primary afferents were mapped using artificial dipole-stimuli presented at 3 dB above the threshold, at a 2 mm distance from the skin surface. Details on the experimental methods employed in these unpublished experiments as well as the following central recordings can be found in Engelmann et al. (2006).

An example of a receptive field is shown as a greyscale 2D-plot in Fig. 13a. Receptive fields of afferents are organised in a simple way with a single centre region and an average extension of 5.2 mm^2 ($n = 12$). Thresholds for evoking an afferent spike (t test: $T = 0.95$, $df = 31$, $p = 0.35$; Fig. 13b) and the maximal width of the receptive fields (t test: $T = 0.1.66$, $df = 26$, $p = 0.12$; Fig. 13c) did not differ between the nasal region and the chin appendage. Similar measures were obtained for trunk afferents (mean width 5.31±2.4 mm, mean threshold 48 ± 2.45μ A, $n = 5$; $p > 0.28$). Thus, although anatomical differences exist between receptors of the foveal and trunk regions (Bacelo and Grant 2001; Bell et al. 1989; Hollmann and von der Emde 2004), the size of individual primary afferent receptive fields appears to be very similar. These data strengthen the idea that the *electro-acuity* at the chin appendage and head region is higher due to the greater receptor density in these regions, which is about five times that found in the trunk region.

We now turn to the organisation of the central representation of the peripheral world. The size and organisation of the receptive fields of the ELL neurons will influence the processing of spatial information, as has been documented in several vertebrate sensory systems (Adelman et al. 2003; Bastian et al. 2002; Catania and Kaas 1997; Lewis and Maler 2001; Mountcastle and Darian-Smith 1974; Ratcliff 1965; Sachdev and Catania 2002).

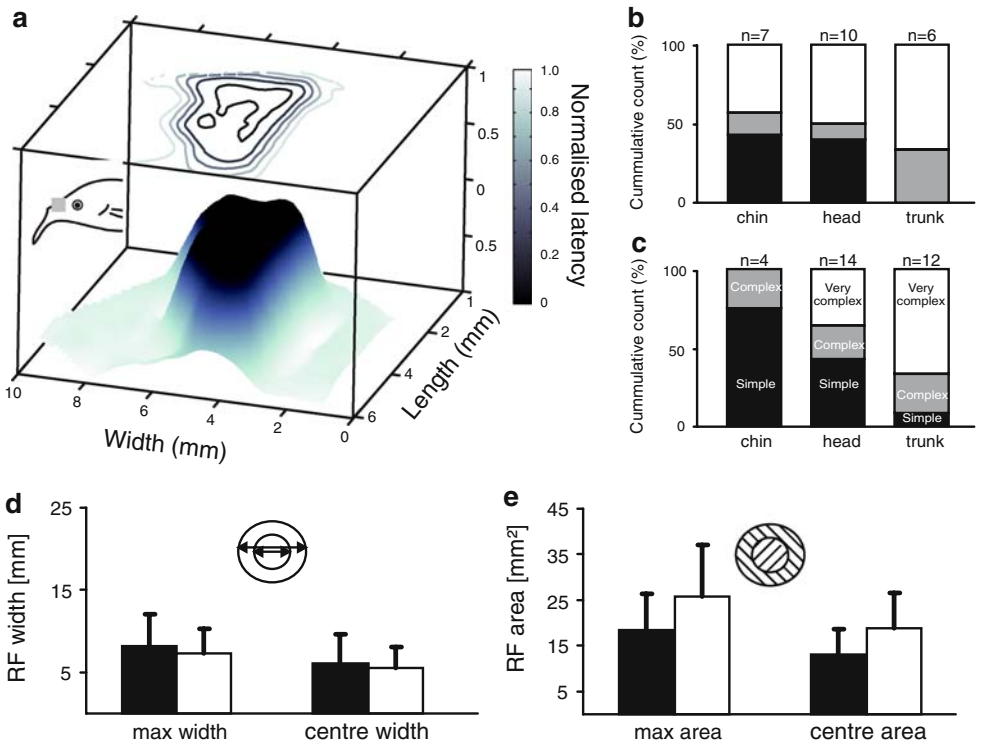

Fig. 14 Receptive fields in ELL and the relative distribution of their complexity. **a** Example of the receptive field based on the first spike latency of an I-cell with a simple receptive field. Latency in this figure was normalised with respect to the maximal latency. The location of the receptive field is indicated by the *grey region* superimposed on the fish-head to the left. **b** Distribution of receptive field complexity for I-cells. **c**Distribution of receptive field complexity for E-cells. Note that in both populations the parameter "complexity" increases from rostral to caudal positions. **d** Mean width of receptive fields recorded in ELL for neurones excited by stimulation of their centre (C-cells, *white bars*) and cells inhibited by stimulation in their centre (*black bars*). **e** The mean area of receptive fields for neurones excited by stimulation of their centre (C-cells, *white bars*) and cells inhibited by stimulation in their centre (*black bars*)

Regardless of the exact algorithm fish use to measure the distance to objects, they will need to extract two cues: a parameter related to the width of the electric image and one related to the location of the peak of the image (Rasnow 1996). As shown above, both parameters are contained in the latencies of the primary afferent spikes, but need to be extracted centrally. The accuracy with which distance, elevation and azimuth of an object can be derived from a single neuron and a population of neurones has been estimated (Lewis and Maler 2001). These authors suggested that an ensemble of neurones codes for spatial parameters. Within a network of neurones, they showed that small receptive fields are best suited to determine the slope of the electric image. Wide receptive fields, however, were found to improve the determination of the peak amplitude of the electric image, a notion going back to Baldi and Heiligenberg (Baldi and Heiligenberg 1988). The above considerations are based on the idea of population coding. In line with this idea, the ELL is topographically mapped in a way that nearby positions in the sensory world have similar representations in the neural population. Such an organisation is likely to be very efficient in the evaluation of the information stored in the population. In summary, *electro-acuity* is linked to the organisation of the central representation of the sensory world.

In our central recordings, we conducted experiments similar to those designed to explore the electrosensory periphery, using an artificial dipole stimulus at 3dB above threshold. We found no correlation of the width and area of the receptive fields with the location of the receptive fields on the fish's body ($n = 53$ extra- and 18 intracellular recordings). Receptive fields were of equal sizes all along the fish's body, including the foveal regions (Fig. 14).

In contrast to the periphery, cells in the ELL can be inhibited (I-cells) or excited (E-cells) by the stimulus. The spatial dimensions of receptive fields of both classes of cells were comparable. For E-cells the average width of receptive fields was 7.3 ± 2.99 mm ($n = 33$) and the mean area $25.85 \pm 11.2\,\text{mm}^2$ ($n = 17$) (see Fig. 14d, e). Comparable measures were determined from I-cells: 8.4 ± 3.8 mm ($n = 19$) and $17.6 \pm 8.2\,\text{mm}^2$ ($n = 9$), respectively. Thus, receptive fields in the ELL of *Gnathonemus* are roughly one order of magnitude smaller than those found in *Apteronotus leptorhynchus* (Bastian 1981b; Bastian et al. 2002). This comparison of sizes depends on the way stimuli have been presented:

Bastian estimated the strength of the dipole to be 1 mV/cm at a lateral distance of 2 mm. This is comparable to the field strength in our data that was 2.4 mV/cm (1 mV/cm s.d.) on average. Interestingly, the sizes of the afferent receptive fields in *Apteronotus* (Bastian 1981a) are comparable to the size we determined in *Gnathonemus petersii* (see above). Hence the roughly fivefold increase of receptive field size area from the periphery to the ELL in *Gnathonemus* suggests that less afferents (one to five, depending on the relative densities of 2–20 mormyromasts/mm^2) converge on an ELL neurone. Such convergence is usually associated with an increase in sensitivity at the cost of spatial resolution (McCreery 1977). The decrease in spatial resolution however would be relatively negligible given that central and peripheral receptive fields are rather small in *Gnathonemus*.

Assuming coding similar to that suggested by Lewis and Maler (2001), the small-sized organisation of the receptive fields in the ELL indicates that they are best suited to extract the distance to an object, but might be less useful in extracting information on the peak-location. Preliminary results from recordings of neurones of the torus semicircularis (T. Röver, personal communication) suggest that wide receptive fields are present at this level. This suggests that high spatial resolution is preserved at the ELL and wide-field receptive fields in the midbrain could extract the location of the image peak.

In contrast to primary afferents (see Fig. 13), receptive fields of neurons in the ELL can be either simple or have a more or less complex centre-surround organization (Bastian 1975; Bell et al. 1997b). Simple receptive fields have a single uniform centre area, whereas complex receptive fields have an antagonistic centre-surround organisation. Units with multiple centre and surrounding areas were classified as complex. Complexity increased from rostral to caudal (Fig. 14b, c). Simple and complex receptive fields, i.e. receptive fields with one centre region, with or without an antagonistic surround, were abundant at the chin appendage and the head, but decreased towards the trunk. In contrast, very complex receptive fields, i.e., fields with more then two excitatory centres that could be surrounded by regions of inhibition or no response above the no-stimulus condition, were dominant in the caudal parts of the fish. Complex receptive fields might enhance the spatial contrast in a way similar to that used in the visual system (Sherman 1979). In general complex receptive fields are well suited for extracting information about the spatial organization of sensory images. The centre-surround interactions can amplify responses to spatial differences, and suppress the responses to uniform image regions. Thereby they can enhance contours in sensory images, acting as Gabor filters. This makes them sensitive to spatial or temporal variations, which convey important information about the environment.

In line with the above reasoning, complex receptive fields encountered on the trunk could be specifically useful for detecting small objects that move with respect to the sensory surface, because motion will cause systematic variations in the spatiotemporal domain. Experimental data on motion and its encoding, however, is currently lacking. Recent modelling studies (Babineau et al. 2007) indicate that motion might be of importance for the discrimination of small objects in front of complex backgrounds similar to the figure-ground problem in vision. Indeed the behavioural experiments (described above) have shown that *Gnathonemus* is able to solve this problem without difficulty when forced to discriminate between objects in the presence of a metal plate in the background (see Fig. 6a).

5 Conclusions

We have investigated the constraints on orientation with the active electric sense going from the pre-receptor and physical level up to the sensory transduction of electrical images and their central representation. Our aim has been both to extend our knowledge of sensory processing in electric fish and to emphasise the physical and behavioural constraints that can lead to ambiguities in electrolocation. With respect to these ambiguities we have indicated some solutions to resolve them, yet quite a number of the issues we addressed still need to be explored in greater detail.

From our behavioural data we conclude that fish are able to determine the distances to objects, although they can confuse spherical and cubic objects whose electric images change slightly differently with distance (Fig. 1c). The latter strongly supports the idea that the parameter used to do this is the slope-amplitude ratio. However, the finding that fish can learn to compensate for the ambiguities between spheres and cubes (von der Emde et al. 1998) shows that they must use additional parameters of the electric image to do so. Irrespective of which parameter fish do use to determine distance, this measure will have an additional ambiguity that arises from the finding that the electric image of a given object changes along the rostro-caudal length of the animals (Babineau et al. 2007). This is also the case in *Gnathonemus* where we recently found that the slope/amplitude ratios at the head region are opposite to those at the trunk (Pusch et al. 2008). This suggests future behavioural experiments to selectively investigate whether fish use the foveal regions for exact distance determination and the trunk in other behavioural contexts or whether they are capable of compensating for the ambiguities caused by these phenomena. In the behavioural work, we have presented here, we establish that *Gnathonemus* can distinguish objects of different size irrespective of their relative distance. They in fact possess the capability of distinguish objects based just on their contours. Modelling the electric images of such objects and measuring the images should enable us to better understand the cues fish use for shape-discrimination.

With regard to complex electrosensory scenes, our data show that when multiple objects are present electric images superimpose, and that this increases ambiguity for discrimination when the objects are close to one another (Fig. 5). Nevertheless, fish can solve discrimination tasks under such conditions (Fig. 6a) and it is clear that further experiments will need to address the acuity of the electric sense in complex electrosensory scenes. How the problem of the convergence of electrical images in apposition and superposition is being solved is unclear. As shown in the section on the interaction between the body of the animal and the field, fish may use exploratory movements to modify the field in a goal-directed manner. Thus, by either determining the spatio-temporal changes of electric images while swimming past them (Babineau et al. 2007), or by manipulating the position of the energy source in a *searchlight* manner, the animals might extract the information necessary for solving the figure-ground problem.

Pre-receptor mechanisms and morphological adaptations play a crucial role in electroreception. The idea that the head of the fish is an electrosensorial fovea due to the high receptor density and the over-representation in the brain (Fig. 12) is supported by the pre-receptor mechanisms that optimise the electric field parameters in this region (Fig. 2). Scanning movements of the chin appendage are an important behavioural strategy during foraging (see supplementary material). For this particular case, we have shown that the pre-receptor mechanisms constitute an elegant way to avoid ambiguities, by moving the field along with the chin (Fig. 3). This means that the chin acts like an electric searchlight, by actively illuminating objects of interest. Again, the funnelling effect is crucial for this phenomenon.

Another important factor that arises due to the interaction between electric images and the water/body interface (Fig. 4) is the formation of electric images with a *Mexican-hat* profile. Because the electric image is a distributed image, where a single point in the environment influences a finite two-dimmensional region on the animals' skin, the *Mexican-hat* profile gives contrast at the sensory surface itself. Presumably that this should be beneficial in electrolocation as it enhances the contrast in this blurred sense and our data on primary afferents does confirm that the *Mexican-hat* profile is maintained within the afferents spike latencies.

Concerning ambiguities due to swimming, we have shown that the relative changes in the local EOD amplitudes are well within the range of modulations that would be caused by relatively big objects in the electrosensory scenery (Fig. 10). Here, no compensation based on pre-receptor mechanisms was found. Instead we can show that the peripheral sensory system does relay ambiguous information to the brain, such that the coding of electric image properties will depend on the current behavioural context (motion, Fig. 11). In order to resolve this problem, fish must compute a normalised electric image. One possibility is that sensory feedback could be used to cancel out the changes produced by the fish's own movement, and proof of such mechanisms has been obtained in Gymnotiform fishes (Bastian 1995). Recent data, however, are in favour of a gain-controlled mechanism where local inhibitory interneurones in the ELL will regulate their inhibitory drive to efferent cells in relation to the strength of the local EOD. The relative balance of excitatory and inhibitory input is thus maintained, resulting in a normalised representation of electric images in these cells (Bacelo et al, in preparation).

One role of the well-documented corollary discharge effects in sensory processing of the ELL (Bell et al. 1997a) could be the resolution of the ambiguities that arise due to the superposition nature of electric images (Rother et al. 2003). Superposition will lead to problems in the discrimination of multiple nearby objects (Fig. 5) because there are no coherent parameters the animal can extract from the "combined images". However, these ambiguities might be resolved using cues derived by moving relative to the objects. This will give rise to spatial and temporal correlations in the electric images which should enable the animals to reconstruct detailed electrosensory scenes. We speculate that in order to obtain the necessary spatial correlations, the adaptive properties of the ELL and the extensive feedback projections from cerebellar and sensory brain regions will be of importance, since they will enable comparison of recent sensory past and current input (Bell 2001).

The central representation of the electrosensory periphery shows a strong magnification of the foveal regions (Fig. 12). Interestingly, we found differences in this magnification for the sensory pathway devoted to waveform detection and the amplitude pathway. Although we focussed on the latter system in this paper, this differentiation indicates that the chin appendage is especially important for waveform analysis. As mentioned in the behavioural section, the discrimination of capacitances can be compared to colour as a separate *qualia* in the electrosensory world. This might be of importance in orienting tasks, allowing a simple distinction between living and non-living objects. For such distinctions, the local EOD in the head region is ideal as no significant phase shifts are present within this region. However the claim that the chin appendage is particularly devoted to waveform detection requires further experimental confirmation, but unpublished work on waveform analysis in the ELL indicates that information on the electric impedance is being computed already at the ELL-level (Fechner and Engelmann, unpublished).

In contrast to the other electric fish where the spatial properties of receptive fields have been studied (Bastian 1975), receptive fields of *Gnathonemus* are small. Thus we speculate that the spatial acuity of the electric sense in this fish might be enhanced. Again, this needs experimental verification. At present studies on the non-classical receptive fields and the

effect of stimulation in the surround (Chacron et al. 2003) are lacking in *Gnathonemus*. While we do not expect to find tuning in ELL neurones of *Gnathonemus* to communication and electrolocation signals as in *Apteronotus* (Bastian et al. 2002; Chacron et al. 2003), non-classical receptive fields have been attributed to improvement of feature extraction in complex sensory environments (Petkov and Subramanian 2007) and might also be present in Mormyrids.

Acknowledgments This work was supported by a Marie Curie Fellowship from the European Commission to J.E. (QLK6-CT-2002-5172), grants from the German Science Foundation (DFG, EN 826/1-1; Em 43/11-1,2,3) and the French Ministry of Foreign Affairs (ECOS-sud; U03B01). R.P is supported by a fellowship from the Friedrich-Ebert-Foundation.

Additional Online Material

Avi1: Fish exploring a 4×4 cm plastic cube that had been placed in the tank 10 s before the movie starts. The sequence is 77 s long; during this time the acquisition of digital images was triggered by the animals own EOD. The relationship between EOD-frequency and the position of the animal in the tank is shown in Fig. 7a. Note the use of both the head and chin appendage as well as the trunk during exploration. During exploration and swimming the tail movements, and hence the changes in the electric field amplitude, can be large. Avi2: High-speed movie of an exploratory saccade-like scanning movement of the Schnauzenorgan. The original sequence was filmed at 128 frames/sec and has been slowed down to 15 frames/sec. The angular velocity in this example was 480°/sec. Avi3: Short sequence of a fish exploring a plastic cylinder seen both in a side- and top-view. The movie is filmed at a rate of 30 frames/sec and the EODs are made audible following 48 kHz digitisation (kindly provided by Michael Hollmann and Sebastian Schäfer). Note that the fish almost exclusively uses the chin appendage while exploring the object. In contrast to Avi1, the object had been explored by the fish previously.

References

Adelman TL, Bialek W, Olberg RM (2003) The information content of receptive fields. Neuron 40:823–833

Assad C (1997) Electric field maps and boundary element simulations of electrolocation in weakly electric fish. Electrical Engineering, California Institute of Technology, Pasadena

Azzopardi P, Cowey A (1993) Preferential representation of the fovea in the primary visual cortex. Nature 361:719–721

Babineau D, Longtin A, Lewis JE (2006) Modelling the field of weakly electric fish. J Exp Biol 209:3636–3651

Babineau D, Lewis JE, Longtin A (2007) Spatial acuity and prey detection in weakly electric fish. PLoS Comput Biol 3:e38

Bacelo J (2007) Sensory processing in the Electrosensory Lobe of the weakly electric fish Gnathonemus petersii. THESE DE DOCTORAT DE L'UNIVERSITE PARIS 6, Pierre et Marie Curie. Paris 6, Paris, p 167

Bacelo J, Grant K (2001) Electrosensory and trigeminal innervation of the Schnauzenorgan in Gnathonemus petersii. In: 6th international congress of neuroethology, Bonn/Germany, p 225

Baldi P, Heiligenberg W (1988) How sensory maps could enhance resolution through ordered arrangements of broadly tuned receivers. Un Ensemble de courbes qui font monter une droite. Biol Cybern 59:313–318

Bastian J (1975) Receptive fields of cerebellar cells receiving exteroceptive input in a ymnotid fish. J Neurophysiol 38:285–300

Bastian J (1981a) Electrolocation: I. How the electroreceptors of Apteronotus albifrons code for moving objects and other electric stimuli. J Comp Physiol A 144:465–479

Bastian J (1981b) Electrolocation: II. The effects of moving objects and other electric stimuli on the activities of two categories of posterior lateral line lobe cells in Apteronotus albifrons. J Comp Physiol A 144:481–494

Bastian J (1995) Pyramidal-cell plasticity in weakly electric fish: a mechanism for attenuating responses to reafferent electrosensory inputs. J Comp Physiol A 176:63–73

Bastian J, Chacron MJ, Maler L (2002) Receptive field organization determines pyramidal cell stimulus-encoding capability and spatial stimulus selectivity. J Neurosci 22:4577–4590

Bell CC (1981) An efference copy which is modified by reafferent input. Science 214(4519):450–453

Bell CC (1990) Mormyromast electroreceptor organs and their afferent fibers in mormyrid fish. II. Intra-axonal recordings show initial stages of central processing. J Neurophysiol 63:303–318

Bell CC (2001) Memory-based expectations in electrosensory systems. Curr Opin Neurobiol 11:481–487

Bell CC, Zakon H, Finger TE (1989) Mormyromast electroreceptor organs and their afferent fibers in mormyrid fish: I. Morphology. J Comp Neurol 286:391–407

Bell CC, Bodznick D, Montgomery JC, Bastian J (1997a) The generation and subtraction of sensory expectations within cerebellum-like structures. Brain Behav Evol 50:17–31

Bell CC, Caputi A, Grant K (1997b) Physiology and plasticity of morphologically identified cells in the mormyrid electrosensory lobe. J Neurosci 17:6409–6423

Budelli R, Caputi AA (2000) The electric image in weakly electric fish: perception of objects of complex impedance. J Exp Biol 203(Pt 3):481–492

Caputi AA (2004) Contributions of electric fish to the understanding of sensory processing by reafferent systems. J Physiol Paris 98:81–97

Caputi AA, Budelli R (2006) Peripheral electrosensory imaging by weakly electric fish. J Comp Physiol A Neuroethol Sens Neural Behav Physiol 192(6):587–600

Caputi AA, Budelli R, Grant K, Bell CC (1998) The electric image in weakly electric fish: physical images of resistive objects in Gnathonemus petersii. J Exp Biol 201(Pt 14):2115–2128

Catania KC (1999) A nose that looks like a hand and acts like an eye: the unusual mechanosensory system of the star-nosed mole. J Comp Physiol A 185:367–372

Catania KC, Kaas JH (1997) Somatosensory fovea in the star-nosed mole: behavioral use of the star in relation to innervation patterns and cortical representation. J Comp Neurol 387:215–233

Castelló ME, Caputi AA, Trujillo-Cenóz O (1998) Structural and functional aspects of the fast electrosensory pathway in the electrosensory lateral line lobe of the pulse fish Gymnotus carapo. J Comp Neurol 401:549–563

Castelló ME, Aguilera PA, Trujillo-Cenoz O, Caputi AA (2000) Electroreception in Gymnotus carapo: Pre-receptional mechanisms and distribution of electroreceptor types. J Exp Biol 203:3279–3287

Chacron MJ, Doiron B, Maler L, Longtin A, Bastian J (2003) Non-classical receptive field mediates switch in a sensory neuron's frequency tuning. Nature 423:77–81

Chen L, House JL, Krahe R, Nelson ME (2005) Modeling signal and background components of electrosensory scenes. J comp Physiol A 191:331–345

Ciali S, Gordon J, Moller P (1997) Spectral sensitivity of the weakly discharging electric fish Gnathonemus petersii using its electric organ discharges as the response measure. J Fish Biology 50:1074–1087

Ćurčić-Blake B, van Netten SM (2006) Source location encoding in the fish lateral line canal. J Exp Biol 209:1548–1559

Douglas RH, Eva J, Guttridge N (1988) Size constancy in goldfish (Carassius auratus). Behav Brain Res 30:37–42

Egelhaaf M, Boddeker N, Kern R, Kretzberg J, Lindemann JP, Warzecha AK (2003) Visually guided orientation in flies: case studies in computational neuroethology. J Comp Physiol A Neuroethol Sens Neural Behav Physiol 189:401–409

Gomez L, Budelli R, Grant K, Caputi AA (2004) Pre-receptor profile of sensory images and primary afferent neuronal representation in the mormyrid electrosensory system. J Exp Biol 207:2443–2453

Goulet J, Engelmann J, Chagnaud B, Franosch JM, Suttner MD, van Hemmen JL (2007) Object localization through the lateral line system of fish: theory and experiment. J Com Physiol A 194(1):1–17

Harder W, Schief A, Uhlemann H (1967) Zur empfindlichkeit des schwachelektrischen Fisches Gnathonemus petersii (Mormyriformes; Teleostei) gegenüber elektrischen Feldern. Z Vergl Physiol 54:89–108

Heiligenberg W (1973) Electrolocation of objects in the electric fish Eigenmannia (Rhamphichthyidae, Gymnotoidei). J Comp Physiol 87:137–164

Heiligenberg W (1977) Principles of electrolocation and jamming avoidance in electric fish. A neuroethological approach. In: Braitenberg V (ed) Studies of brain function. Springer Verlag, Berlin, pp 1–85

Hollmann M, von der Emde G (2004) Two electrical foveae in the skin of the weakly electric fish, Gnathonemus persii (Teleostei). 97 Jahresversammlung der Deutschen Zoologischen Gesellschaft, Rostock, p P14

Hollmann M, von der Emde G (2007) Electrofoveal regions on the skin of a weakly electric fish. 8th Int Congress of Neuroethology, Vancouver, Canada

Jeffress LA (1948) A place theory of sound localization. J Comp Physiol Psychol 41:35–39

Kalmijn AJ (1974) The detection of electric fields from inanimate and animate sources other than electric organs. In: Fessard A (ed) Handbook of sensory physiology. Springer, Berlin, pp 148–200

Karmeier K, van Hateren JH, Kern R, Egelhaaf M (2006) Encoding of naturalistic optic flow by a population of blowfly motion-sensitive neurons. J Neurophysiol 96:1602–1614

Landsberger M, von der Emde G (2007) Relevance of a peculiar retina type for visual detection in the weakly electric elephantnose fish. In: Eigth international conference of neuroethology, Vancouver/Canada, p PO37

Leibowitz HW (1971) Sensory, learned, and cognitive mechanisms of size perception. Ann NY Acad Sci 188:47–60

Lewis JE, Maler L (2001) Neuronal population codes and the perception of object distance in weakly electric fish. J Neurosci 21:2842–2850

Lissmann HW (1958) On the function and evolution of electric organs in fish. J Exp Biol 35:156–191

Lissmann HW, Machin KE (1958) The mechanism of object location in Gymnarchus niloticus and similar fish. J Exp Biol 35:451–486

McCreery DB (1977) Spatial organization of receptive fields of lateral lemniscus neurons of the lateral line lobe of the catfish Ictalurus nebulosus. J Comp Physiol A 113:341–353

Migliaro A, Caputi AA, Budelli R (2005) Theoretical analysis of prereceptor image conditioning in weakly electric fish. PLoS Comp Biol 1:123–131

Mountcastle V, Darian-Smith I (1974) Neuronal mechanisms in somesthesia. CV Mosby Company, Mosby

Pereira ASF, Centurión V, Caputi AA (2005) Contextual effects of small environments on the electric images of objects and their brain evoked responses in weakly electric fish. J Exp Biol 208:961–972

Petkov N, Subramanian E (2007) Motion detection, noise reduction, texture suppression, and contour enhancement by spatiotemporal Gabor filters with surround inhibition. Biol Cybern doi:10.1007/s00422-007-0182-0

Pusch R, von der Emde G, Hollmann M, Bacelo J, Nöbel S, Grant K, Engelmann J (2008) Active Sensing in a Mormyrid Fish – Electric Images and Peripheral Modifications of the Signal Carrier give Evidence of Dual Foveation. J Exp Biol 211:921–934

Quinet P (1971) Etude systematique des organes sensoriels de la peau des Mormyriformes (Pisces, Mormyriformes). Ann Mus R Afr Cent Tervuren (Belg) Ser 8(190):1–97

Rasnow B (1996) The effects of simple objects on the electric field of Apteronotus. J Com Physiol A 178:397–411

Ratcliff F (1965) Mach bands: quantitative studies on neuronal structures in the retina. Holden Day, San Francisco

Rother D (2003) Simulación de Imágenes Eléctricas en Peces Eléctricos de Descarga Débil. Simulación de Imágenes Eléctricas en Peces Eléctricos de Descarga Débil. Universidad de la República, Montevideo, p 93

Rother D, Migliaro A, Canetti R, Gomez L, Caputi A, Budelli R (2003) Electric images of two low resistance objects in weakly electric fish. Biosystems 71:169–177

Sachdev RN, Catania KC (2002) Receptive fields and response properties of neurons in the star-nosed mole's somatosensory fovea. J Neurophysiol 87:2602–2611

Sawtell NB, Williams A, Roberts PD, von der Emde G, Bell CC (2006) Effects of sensing behavior on a latency code. J Neurosci 26:8221–8234

Schuster S, Amtsfeld S (2002) Template-matching describes visual pattern-recognition tasks in the weakly electric fish Gnathonemus petersii. J Exp Biol 205:549–557

Schwarz S, von der Emde G (2001) Distance discrimination during active electrolocation in the weakly electric fish Gnathonemus petersii. J Comp Physiol A 186:1185–1197

Sherman SM (1979) Functional-significance of *X* and *Y* cells in normal and visually deprived cats. Trends Neurosci 2:192–195

Sicardi EA, Caputi AA, Budelli R (2000) Physical basis of distance discrimination in weakly electric fish. Physica A 86–93

Szabo T, Hagiwara S (1967) A latency change mechanism involved in sensory coding of electric fish (mormyrids). Physiol Behav 2:331–335

von der Emde G (2006) Non-visual environmental imaging and object detection through active electrolocation in weakly electric fish. J Comp Physiol A Neuroethol Sens Neural Behav Physiol 192(6):601–612

von der Emde G, Ronacher B (1994) Perception of electric properties of objects in electrolocating weakly electric fish: two-dimensional similarity scaling reveals a City-Block metric. J Comp Physiol A 175:801–812

von der Emde G, Fetz S (2007) Distance, shape and more: Recognition of object features during active electrolocation in a weakly electric fish. J Exp Biology 210:3082–3095

von der Emde G, Schwarz S, Gomez L, Budelli R, Grant K (1998) Electric fish measure distance in the dark. Nature 395:890–894

Wagner HJ (2007) Bipolar Cells in the "Grouped Retina" of the Elephantnose Fish (Gnathonemus petersii). Vis Neurosci 24(3):355–362